# Binding and Selectivity in L-Type Calcium Channels: A Mean Spherical Approximation

Wolfgang Nonner,* Luigi Catacuzzeno,* and Bob Eisenberg†

*Department of Physiology and Biophysics, University of Miami School of Medicine, Miami, Florida 33101-4819; and †Department of Molecular Biophysics and Physiology, Rush Medical College, Chicago, Illinois 60612 USA

ABSTRACT L-type calcium channels are $Ca^{2+}$ binding proteins of great biological importance. They generate an essential intracellular signal of living cells by allowing $Ca^{2+}$ ions to move across the lipid membrane into the cell, thereby selecting an ion that is in low extracellular abundance. Their mechanism of selection involves four carboxylate groups, containing eight oxygen ions, that belong to the side chains of the "EEEE" locus of the channel protein, a setting similar to that found in many $Ca^{2+}$-chelating molecules. This study examines the hypothesis that selectivity in this locus is determined by mutual electrostatic screening and volume exclusion between ions and carboxylate oxygens of finite diameters. In this model, the eight half-charged oxygens of the tethered carboxylate groups of the protein are confined to a subvolume of the pore (the "filter"), but interact spontaneously with their mobile counterions as ions interact in concentrated bulk solutions. The mean spherical approximation (MSA) is used to predict ion-specific excess chemical potentials in the filter and baths. The theory is calibrated using a single experimental observation, concerning the apparent dissociation constant of $Ca^{2+}$ in the presence of a physiological concentration of NaCl. When ions are assigned their independently known crystal diameters and the carboxylate oxygens are constrained, e.g., to a volume of 0.375 $nm^3$ in an environment with an effective dielectric coefficient of 63.5, the hypothesized selectivity filter produces the shape of the calcium binding curves observed in experiment, and it predicts $Ba^{2+}/Ca^{2+}$ and $Na^+/Li^+$ competition, and $Cl^-$ exclusion as observed. The selectivities for $Na^+$, $Ca^{2+}$, $Ba^{2+}$, other alkali metal ions, and $Cl^-$ thus can be predicted by volume exclusion and electrostatic screening alone. Spontaneous coordination of ions and carboxylates can produce a wide range of $Ca^{2+}$ selectivities, depending on the volume density of carboxylate groups and the permittivity in the locus. A specific three-dimensional structure of atoms at the binding site is not needed to explain $Ca^{2+}$ selectivity.

## INTRODUCTION

$Ca^{2+}$ binding proteins of high specificity are used by cells to control vital intracellular processes, and transmembrane proteins with a hole down their middle (calcium channels) generate $Ca^{2+}$ signals by regulating the movement of $Ca^{2+}$ into the cell. These proteins specifically accumulate $Ca^{2+}$ from a large excess of other ions into a binding site that includes a cluster of carboxylate groups. Carboxylate groups are provided by adjacent aspartate or glutamate residues, e.g., the "EEEE locus" of calcium channels (Heinemann et al., 1992; Mikala et al., 1993; Yang et al., 1993; Ellinor et al., 1995), or the "EF hand" motif found in many $Ca^{2+}$ regulated proteins (reviewed by Nelson and Chazin, 1998). A cluster of tethered carboxylate groups is found also in $Ca^{2+}$ chelating compounds, such as EGTA. $Ca^{2+}$ specific binding thus seems to arise as a generic property of carboxylate clusters.

The selectivity of L-type calcium channels depends on the solutions bathing them. Although these channels conduct $Ca^{2+}$ in the presence of a hundredfold excess of alkali cations (Reuter and Scholz, 1977; Lee and Tsien, 1984), they can pass large currents of monovalent cations when divalent ions are absent (Kostyuk et al., 1983; Almers and McCleskey, 1984). They accept cations as large as tetramethylammonium (TMA; McCleskey and Almers, 1985) suggesting to Almers and McCleskey a relatively wide aqueous pore with specificity arising from unknown chemical interactions in "calcium-binding pockets."

The idea of localized binding sites, or pockets, has been the basis of chemical kinetic descriptions of ionic conduction in calcium channels (Hille and Schwartz, 1978; Almers and McCleskey, 1984; Hess and Tsien, 1984; Dang and McCleskey, 1998). Ions are viewed as hopping between discrete binding sites formed by a specific arrangement of the atoms of the protein (Miller, 1999). The interactions of ions with binding sites are quantified by free enthalpies assumed to be independent of the ionic densities in the solutions around the channel. The sites are thought to bind ions in 1:1 stoichiometry, such that a site either is vacant or holds one univalent or one divalent cation. The electrical charge now known to be an integral part of the selectivity filter was not included in these kinetic models, and so electrical energy and forces between the filter and conducted ions were treated vaguely, if at all.

Here, we approach the problem of $Ca^{2+}$-specific binding by considering two forces that are *both necessarily* involved in determining permeation, the short-range core-core repulsion of ionic spheres that determine the "goodness of fit" between permeating ion and channel protein (Armstrong, 1989), and the long-range electrical force (Eisenman and Horn, 1983) acting on those spheres. In this model, selectivity is determined by the balance of these forces.

*Received for publication 28 February 2000 and in final form 12 June 2000.*

Address reprint requests to Dr. Robert S. Eisenberg, Dept. of Molecular Biophysics, Rush Medical Center, 1750 W. Harrison St., Chicago, IL 60612-3824. Tel.: 312-942-6467; Fax: 312-942-8711; E-mail: beisenbe@rush.edu.



0006-3495/00/10/1976/17 $2.00

Ionic specificity is computed in our model in a hypothesized setting of minimal structure. Ions and carboxylate groups are assumed to associate like charged molecules of a homogeneous fluid without predefined structure. Electrostatic and excluded volume interactions are described by the primitive MSA (mean spherical approximation) model of electrolytes (Blum, 1975; Triolo et al., 1976, 1978a, 1978b; Blum and Hoye, 1977; Simonin et al., 1996, 1998; Simonin, 1997) that describes the activity coefficient of ionic solutions from infinite dilution to saturation and is even useful in anhydrous melts of pure salt (Boda et al., 1999).

We use the MSA as an approximation that is analytical and hence easy to compute and understand physically. The particular theory used to describe electrostatic and core-core repulsive forces is not central to our theme: other theories will be used in future work, no doubt. The central theme is that electrostatics and core-core repulsion are enough to explain the essential aspects of physiological selectivity in $Ca^{2+}$ channels. In this view, selectivity among physiological ions springs from the diameters and charges of the selected mobile ions and the selecting carboxylate oxygens of the protein. The protein architecture has surprisingly little role in this view of selectivity; it sets the dielectric coefficient and the volume density of structural oxygen anions and accommodates the resulting mechanical forces. The specific arrangement of atoms in the hypothesized binding arises spontaneously. It is the result, not the cause, of the specified forces. Two parameters—filter volume and dielectric coefficient—can set the $Ca^{2+}$ dissociation constant of the channel over the range from millimolar to subnanomolar, which includes the range found in $Ca^{2+}$ selective channels and $Ca^{2+}$ binding proteins.

## THEORY AND METHODS

Binding of ions to the L-type calcium channel is computed here from a theory that treats the selectivity filter of the channel as an ion exchange "resin" containing negative fixed charge, much as macroscopic theories treated ion exchange membranes some time ago (Teorell, 1953; Helfferich, 1962; Coster et al., 1969; Coster, 1973). The resin and baths are assumed to be at equilibrium, at the same electrochemical potential: the equilibrium equation of state is solved numerically to determine the densities of ions in the resin and the electrical potential there. Previous analysis of a microscopic selectivity filter, using Poisson-Nernst-Planck theory, showed the utility of this approach: when the electrostatic screening length remains short compared to the dimensions of the filter (Nonner and Eisenberg, 1998), a quasi-macroscopic analysis captures most of the behavior of the system (except the anomalous mole fraction effect, see Fig. 3).

We assume that the ion exchanger of the L-type calcium channel is made of the selectivity oxygens of the EEEE locus. The contents of the selectivity filter and the baths are described as the two phases in a Donnan system of classical physiology. The oxygens are described as tethered ions with the same properties as carboxylate ions in bulk, but confined to the subvolume of the selectivity filter. They are assigned a partial charge of $-\frac{1}{2}e_0$ each. Ions such as $Ca^{2+}$, $Na^+$, and $Cl^-$ can move from phase to phase, but the "selectivity oxygens" cannot. The permeating ions and ionized oxygens of the channel assume mean positions that minimize the free energy of the system. The selectivity oxygens are part of this system, but their exact position and that of the permeating ions are *not* predefined by a specific architecture.

Ions bind in, or are excluded from, the filter because the system has a more (or less) favorable free energy when ions are bound than when they are free. The free energy of binding/exclusion involves "ideal" terms, the concentration and electrical terms of the electrochemical potential of an ideal electrolyte solution, but also "excess" terms that arise in real solutions. (The chemical potential of an ion is the change of free energy of the system that occurs when the mean density of the ion is changed by a tiny amount. Note that a chemical potential for a species of ion exists even if that ion is not present in the system, just as an electric potential exists even when no probing charges are present.)

The novel part of our analysis is the computation of the thermodynamic excess properties of ions in the selectivity filter using a statistical mechanical theory of bulk electrolyte solutions, the so-called "primitive" version of the MSA. This theory represents ions as charged hard spheres and water as a continuous dielectric. In the primitive model, the dielectric coefficient (which varies with the composition of the solution) describes the attenuation by water of electrostatic interactions between the ions and some of the interactions of ions with water. The mutual exclusion of the finite ionic volumes and the electrostatic interactions (screening) among the ions produce the non-ideal (excess) components of the chemical potentials. The excess chemical potentials generally are different for different ionic species. No other effects (such as specific interactions between atomic orbitals of $Ca^{2+}$ and the molecular orbitals of the carboxylic groups) are invoked in this model of the selectivity filter.

Inside the selectivity filter, the excess chemical potentials computed by the MSA describe the selective "binding" of ions to the channel protein. In the bath, the excess chemical potentials computed by the MSA establish the reference state from which the channel accumulates ions selectively. In this section, we summarize the computation of excess chemical potentials and other relevant quantities of MSA theory, and describe their use in predicting the partitioning of ions between the bath and the channel.

### The MSA theory

MSA theory derives thermodynamic properties of electrolyte solutions from statistical mechanics. The volume density of the Helmholtz free energy $\Delta A$ is expressed as the sum of ideal and excess contributions.

$$\Delta A = \Delta A^{\mathrm{id}} + \Delta A^{\mathrm{ex}} \tag{1}$$

The excess free energy has two components: 1) excluded volume effects that arise in a solution of uncharged hard spheres, usually called the "hard-sphere" (HS) component $\Delta A^{\mathrm{HS}}$, and 2) electrostatic effects that arise from the mutual screening of charged hard spheres, usually called the "electrostatic" (ES), or sometimes "MSA," component $\Delta A^{\mathrm{ES}}$.

$$\Delta A^{\mathrm{ex}} = \Delta A^{\mathrm{HS}} + \Delta A^{\mathrm{ES}} \tag{2}$$

The hard-sphere effects are entropic and depend on how space can be occupied by spheres. Excluded volume effects of this sort have been included in treatments of excess free energy since the time of van der Waals. Analytical expressions describing the hard-sphere effects have been derived in the Percus-Yevick theory of uncharged liquids (see Mansoori et al., 1971; Salacuse and Stell, 1982; and original references cited in footnotes 5 and 6 of the latter paper). The expressions used will be simply stated below (Eqs. 19–22).

The part of MSA theory that is concerned with the electrostatic interactions among charged spheres of finite diameters is outlined in this section. Hard spheres cannot approach as closely as the point charges approach a central ion in Debye-Hückel theory, and this simple property accounts for a substantial part of the excess electrostatic energy of a solution of hard charged spheres. The electrostatic part of the Helmholtz

free energy density

$$\Delta A^{ES} = \Delta E^{ES} - T\Delta S^{ES} \quad (3)$$

involves $\Delta E^{ES}$, the excess electrostatic energy produced by the ionic charges, and $\Delta S^{ES}$, the excess entropy associated with the screening configurations sought by the ions. $\Delta E^{ES}$ is the sum of the self-energies of each ion and its surrounding ionic cloud, by which the central ion is perfectly screened:

$$\Delta E^{ES} = -\frac{e_0^2}{4\pi\varepsilon\varepsilon_0}\sum_i \rho_i\left(\frac{z_i^2}{\sigma_i + 1/\Gamma} + \frac{z_i\eta\sigma_i/\Gamma}{\sigma_i + 1/\Gamma}\right) \quad (4)$$

The form of this equation suggests that the countercharge of ion *i* can be thought of as smeared over a spherical surface that has the diameter $\sigma_i + 1/\Gamma$ and is centered about the ion. Here, $\rho_i$, $\sigma_i$, and $z_i$ are the number density, diameter, and valence of ionic species *i*. $\Gamma$ is the MSA screening parameter, in units of inverse length; $\eta$ is a measure of the difference in diameter of different types of ions (see Eq. 8; $e_0$ is the charge on a proton; $\varepsilon_0$ is the permittivity of the vacuum, and $\varepsilon$ is the relative permittivity of the solvent, i.e., its dielectric "coefficient."

The ES excess entropy is

$$\Delta S^{ES} = -\frac{k_B}{3\pi}\Gamma^3 \quad (5)$$

The variational principle (Blum, 1980; Rosenfeld and Blum, 1986; Blum and Rosenfeld, 1991)

$$\frac{\partial}{\partial\Gamma}\Delta A^{ES} = 0 \quad (6)$$

yields the screening parameter $\Gamma$ from the implicit relation (Blum, 1975; Blum and Hoye, 1977)

$$4\Gamma^2 = \frac{e_0^2}{k_B T\varepsilon\varepsilon_0}\sum_i \rho_i\left[\frac{z_i - \eta\sigma_i^2}{1 + \Gamma\sigma_i}\right]^2 \quad (7)$$

where $k_B$ and $T$ are the Boltzmann constant and absolute temperature, and the MSA parameter $\eta$ represents the effects of nonuniform ionic diameters.

$$\eta = \frac{1}{\Omega}\frac{\pi}{2\Delta}\sum_k \frac{\rho_k\sigma_k z_k}{1 + \Gamma\sigma_k} \quad (8)$$

$\eta$ is zero when all ions have the same diameter, and its effect is small in our calculations: $|\eta\sigma_i^2| < 0.04$. $\Omega$ is determined by

$$\Omega = 1 + \frac{\pi}{2\Delta}\sum_k \frac{\rho_k\sigma_k^3}{1 + \Gamma\sigma_k} \quad (9)$$

$\Delta$ measures the volume fraction *not* filled by ionic hard-spheres:

$$\Delta = 1 - \frac{\pi}{6}\sum_k \rho_k\sigma_k^3 \quad (10)$$

In the limit of point charges ($\sigma_i \to 0$), the MSA screening parameter reduces to

$$4\Gamma^2(\sigma_i \to 0) = \frac{e_0^2}{k_B T\varepsilon\varepsilon_0}\sum_i \rho_i z_i^2 = \kappa^2 \quad (11)$$

where $\kappa$ is the Debye-Hückel screening parameter.

The MSA screening parameter $\Gamma$ is defined in an implicit equation (7), with $\Gamma$ on both sides, and so its computation requires an iterative solution of Eq. 7. The iteration is usually started using the DH screening length as the initial guess $\Gamma^{(0)} = \kappa/2$.

The MSA can be constructed as an interpolation between limiting laws, both of which it describes exactly (Blum and Rosenfeld, 1991):

1. The classical limit described by Debye-Hückel theory, namely low concentration and low ionic charge. Here ion size does not matter, and MSA and Debye-Hückel theory are identical;
2. The Onsager limits. When the ionic concentration goes to infinity and at the same time the ionic charge diverges to infinity, then the limiting energy and free energy is bounded by the energy of the ions encapsulated by a thin metal grounded foil (Onsager, 1939; Rosenfeld and Blum, 1986). In the infinite density and infinite charge limits, free energy is asymptotically equal to the internal (that is, electrostatic) energy, and the entropy term is asymptotically small. This limit is also approached at zero temperature and the limit is sometimes named that way.

MSA theory is a natural extension of DH theory, in which electrostatic interactions among ions are constrained by finite ionic diameters. The results can be stated in analytical form and have a striking formal similarity to those of DH theory (Blum, 1975; Bernard and Blum, 1996; Blum et al., 1996): the excess thermodynamic properties can be expressed as functions of a screening parameter (called $\Gamma$ in MSA), which is analogous to, but numerically different from, the screening parameter $\kappa$ of DH theory. The MSA screening length excluding the radius of the central ion—that is, $(2\Gamma)^{-1}$—is greater than the DH screening length $\kappa^{-1}$, because the finite diameter of ions in the MSA prevents them from approaching as closely as the point charges in DH.

## Excess chemical potentials and osmotic coefficients

The MSA determines the excess chemical potential and osmotic coefficients from the excess free energy $\Delta A^{ex}$. The excess chemical potential $\Delta\mu_i^{ex}$ is computed as two components, one arising from the free energy change due to electrostatic screening (ES component), the other from the pressure work due to the excluded volume of hard spheres (HS component):

$$\Delta\mu_i^{ex} = \Delta\mu_i^{ES} + \Delta\mu_i^{HS} \quad (12)$$

The (molar) osmotic coefficient $\phi$ is also expressed in those components

$$\phi = 1 + \Delta\phi^{ES} + \Delta\phi^{HS} \quad (13)$$

The ES components in these expressions are negative because they arise from the mutual electrostatic attraction of the ions. The HS parts are positive because they are due to the increase of pressure (i.e., mechanical) work arising from the mutual exclusion of the ions of finite diameter. The excess chemical potentials can be positive or negative, depending on which component dominates, and thus can imply a tendency of the solution to "attract" or "repel" ions of the species. Selectivity arises in this way.

MSA derives expressions for the electrostatic parts of the excess chemical potentials and osmotic coefficients using standard thermodynamics (Blum, 1980):

$$\Delta\mu_i^{ES} = \frac{\partial}{\partial\rho_i}\Delta A^{ES} \quad (14)$$

$$\Delta\phi_i^{ES} = \frac{\rho_i}{k_B T}\frac{\partial}{\partial\rho_i}\frac{\Delta A^{ES}}{\rho_i} \quad (15)$$

in which the differentiation is performed at constant $\Gamma$, because of Eq. 6. The results derived from these relations automatically satisfy the Gibbs-Duhem relation that constrains the chemical potentials of all components of a solution, including the solvent.

The explicit expressions for the individual excess chemical potentials and the mean osmotic coefficient are:

$$\Delta\mu_i^{ES} = -\frac{e_0^2}{4\pi\varepsilon\varepsilon_0}\left[\frac{\Gamma z_i^2}{1+\Gamma\sigma_i} + \eta\sigma_i\left(\frac{2z_i - \eta\sigma_i^2}{1+\Gamma\sigma_i} + \frac{\eta\sigma_i^2}{3}\right)\right] \tag{16}$$

$$\Delta\phi^{ES} = -\frac{\Gamma^3}{3\pi\rho_t} - \frac{e_0^2}{4\pi\varepsilon\varepsilon_0 k_B T}\frac{2\eta^2}{\pi\rho_t} \tag{17}$$

$$\rho_t = \sum_k \rho_k \tag{18}$$

The hard-sphere components of the excess chemical potential and of the osmotic coefficient are (Salacuse and Stell, 1982)

$$\Delta\mu_i^{HS} = k_B T\left[\frac{3\xi_2\sigma_i + 3\xi_1\sigma_i^2}{\Delta} + \frac{9\xi_2^2\sigma_i^2}{2\Delta^2} + \xi_0\sigma_i^3(1+\Delta\phi^{HS}) - \ln\Delta\right] \tag{19}$$

$$\Delta\phi^{HS} = \frac{\xi_3}{\Delta} + \frac{3\xi_1\xi_2}{\xi_0\Delta^2} + \frac{3\xi_2^3}{\xi_0\Delta^3} \tag{20}$$

using the geometrical measure variables

$$\xi_n = \frac{\pi}{6}\sum_k \rho_k\sigma_k^n \tag{21}$$

$$\Delta = 1 - \xi_3 \tag{22}$$

The HS components arise solely from a change in entropy that is negative because fewer configurations are available to a solution containing spheres than to a solution containing mass points. The hard-sphere excess free energy density is

$$\Delta A^{HS} = -T\Delta S^{HS} = \sum_i \rho_i\Delta\mu_i^{HS} - \Delta\phi^{HS}k_B T\sum_i \rho_i \tag{23}$$

The osmotic pressure $\Pi$ is determined by the osmotic coefficient $\phi$ and densities

$$\Pi = \phi\cdot k_B T\sum_i \rho_i \tag{24}$$

## Selectivity filter of the calcium channel

Consider a system of two connected compartments, one the selectivity filter containing the selectivity oxygens, the other, the bath remote from the selectivity filter (Fig. 1). The fixed charge of the selectivity oxygens determines the local concentration of mobile ions, chiefly the counterions, $Ca^{2+}$ and $Na^+$. The concentration of ions in the bath far from the selectivity filter is determined by the experimenter. The local concentrations of ions are in equilibrium with the concentration of ions in the bath that is varied in typical experiments, e.g., Fig. 2. Equilibrium is only possible if another force opposes the gradient of concentration between local and remote ions. One other force is the gradient of the long-range electric potential between local and remote locations. The value of this boundary potential or Donnan potential $\Psi$ depends on the concentration of selectivity oxygens and of ions in the bath. Another force comes from the specific local excess chemical potentials that are created by the selectivity filter, and generally differ from those in the bath. We compute the long-range and local binding forces in our theory of selective binding.

We describe the selectivity filter of the L-type calcium channel as a thermodynamic system surrounded by a larger reservoir of controlled composition (the two baths, which are merged in this treatment). Variables describing the filter have no subscripts (for tidiness). The system is at equilibrium so it exchanges heat at the temperature of the reservoir, and it exchanges mobile ions at the chemical potential of the reservoir. Variables describing the baths are marked with the subscript 0 (zero). The equilibrium is defined by the minimum of the "availability function" $\omega$ of Clausius (see p. 92 of Mandl, 1988) that describes the work that can be done by a system in contact with an environment, when certain exchange rules are enforced among them. The function $\omega$ might be also called the grand canonical free energy.

$$\omega = E - T_0 S + P_0 V - \sum_i \mu_{0,i}N_i \tag{25}$$

where $E$ is the internal energy of the system, $T_0$ is the temperature of the baths, $S$ is the entropy of the filter, $P_0$ is the pressure in the bath, $V$ is the volume of the filter, $\mu_{0,i}$ is the chemical potential of component $i$ in the baths, and $N_i$ is the number of molecules of species $i$ in the filter.

The Helmholtz free energy $\underline{A}$ (not the density $A$) in the selectivity filter is

$$\underline{A} = E - T_0 S = \underline{A}^{ex} + k_B T_0\sum_i (N_i\ln\rho_i - N_i) + e_0\Psi\sum_i z_i N_i \tag{26}$$

where $\underline{A}^{ex}$ is the excess free energy (not density) of the molecules in the selectivity filter, $\rho_i$ is the number density ($N_i/V$) of molecules of species $i$ in the filter, and $\Psi$ is the electrical potential (often called the Donnan potential or voltage) of the selectivity filter minus that of the surrounding baths (i.e., reservoir).

At equilibrium the partial derivatives of $\underline{A}$ with respect to the independent variables are all zero, i.e., the partial derivatives with respect to $N_i$ and $\Psi$ are all zero. Setting the partial derivatives with respect to $N_i$ equal to zero implies that the chemical potentials in the baths and selectivity filter are equal, namely

$$\mu_i = \mu_i^0 + \mu_i^{ex} + k_B T\ln\rho_i + e_0 z_i\Phi = \mu_{0,i}^0 + \mu_{0,i}^{ex} + k_B T\ln\rho_{0,i} \tag{27}$$

Setting the partial derivative with respect to electrical potential to zero implies electroneutrality,

$$e_0\sum_i z_i N_i = 0 \tag{28}$$

The selectivity filter of the calcium channel is of atomic dimensions, as are the boundary layers at the interfaces between filter and baths. Our analysis does not account for any mechanical work done on the walls of the channel, nor does it account for electrical energy stored in the capacitance of the boundary layers. The boundary layer is represented in the Donnan system as a jump in electrical potential that generally is present at the interface of the two compartments. In a previous analysis we simulta-

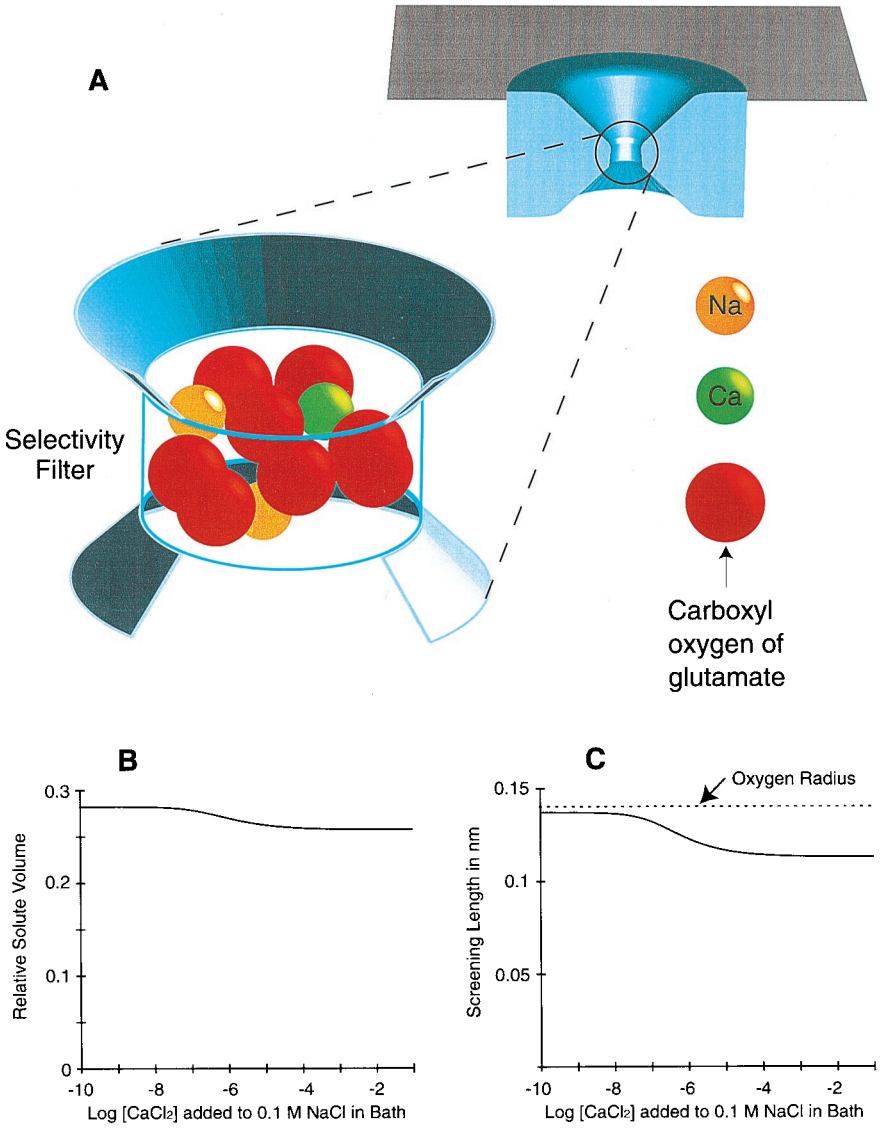


FIGURE 1 (*A*) Schematic view of the hypothesized selectivity filter. The selectivity filter is shown as a cylindrical constriction between wider funnel-like atria of the channel. Filter and ionic dimensions are drawn to scale. The filter contains eight structural oxygen ions that represent the glutamate carboxylate residues of the EEEE locus in the $Ca^{2+}$ channel. Each structural oxygen has an assigned partial charge of $-\frac{1}{2}e_0$. The "selectivity filter" is defined as the subvolume of the pore accessible to these "selectivity" oxygen ions. The MSA theory of this paper is directly concerned with the volume of the filter; the dimensions shown here (0.5 nm axial length, ~1 nm diameter) correspond to a volume of 0.375 $nm^3$. The mobile and oxygen ions in the filter are thought to associate more or less like the ions of a very concentrated bulk solution with no predefined "binding sites" of definite structure. (*B*) Occupied fraction of the filter volume. In this calculation, the bath contained 0.1 M NaCl, and $CaCl_2$ was added to the bath as indicated on the abscissa. The ordinate shows the fraction of the filter volume occupied by structural oxygen ions and the mobile ions that partition from the bath into the filter. Same simulation as in Panel C and Fig. 2 and 3. Substantial excluded volume effects among the ions typically arise when the ions fill more than ¼ of the volume. (*C*) MSA screening length in the filter shown as a function of bath $Ca^{2+}$ added as $CaCl_2$ to a 0.1 M NaCl solution (same simulation as in Panel B and Figs. 2 and 3). The screening length ($1/(2\Gamma)$, see Eqs. 7 and 11), is smaller than the oxygen radius (*dashed line*), and hence substantially smaller than the filter dimensions. The screening length is reduced as divalent $Ca^{2+}$ replaces monovalent $Na^+$ in the filter solution.

neously solved the Poisson and Nernst-Planck equations for a channel geometry (Nonner and Eisenberg, 1998) with essentially similar results. The issue of mechanical work is discussed later in this paper and will be analyzed in a subsequent publication.

## Numerical procedures: solving the Donnan system

The filter and baths are required to have the same electrochemical potential. The resulting equation of state is solved to determine the densities of ions in the filter and the electrical potential there. The inputs of the computation are densities (number per volume) in the bath of the exchangeable ion species, $\rho_{0,i}$, and the density of the tethered carboxyl oxygens in the selectivity filter, $\rho_x$. The outputs of the computation are the densities in the filter of all exchangeable ion species $\rho_i$, the electrical potential in the filter with respect to the bath $\Psi$, measured in units of $k_BT/e_0$, and the excess chemical potentials of all ions species in the bath $\mu_{0,i}^{ex}$ and filter $\mu_i^{ex}$, expressed in units of $k_BT$.

Excess chemical potentials of ions and the Donnan potential depend on the ionic concentrations of all species in each compartment. Conversely, the partitioning into (and hence the concentrations in) the filter compartment depend on the excess chemical potentials and Donnan potential. The ion concentrations in the filter are initially unknown, and so the system needs to be solved by a numerical iteration. The numerical iteration has to be done anew each time the composition of the bath or properties of the selectivity filter are changed.

The MSA equations allow the excess chemical potentials to be very steep functions of concentration. Two numerical safeguards (described below) were found necessary to ensure convergence even in extreme cases; these safeguards limit the iterative pace of change in the excess chemical and electrical potentials.

The plan of the computation was

1. Solve the MSA to compute the excess chemical potentials $\mu_{0,i}^{ex}$ in the baths for the given set of densities of ions in the bath $\rho_{0,i}$;
2. Initialize the estimates of the Donnan potential and excess chemical potentials in the filter. The argument of the functions refers to the iteration number $m$

$$\Psi(0) = 0; \quad \mu_i^{ex}(0) = 0; \tag{29}$$

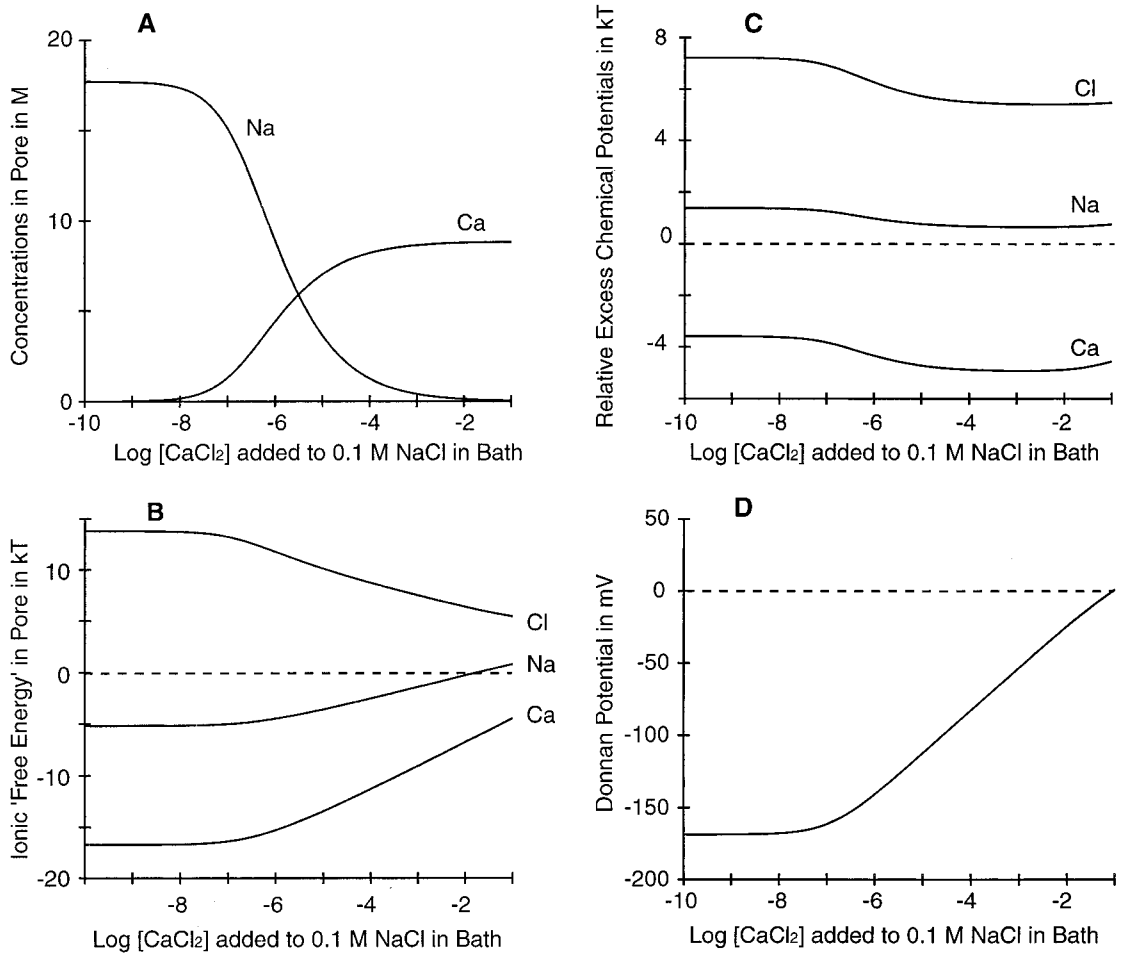


FIGURE 2 $Ca^{2+}$, $Na^+$, and $Cl^-$ selectivities in the hypothesized filter. In a simulated experiment, $CaCl_2$ is added to the 0.1 M NaCl solution so the bath $Ca^{2+}$ concentration is varied from $10^{-10}$ to $10^{-1}$ M while NaCl remains at $10^{-1}$ M. The selectivity filter is described using the standard pore of Fig. 1 *A* and the dielectric coefficient is assigned the value of 63.5. (*A*) Ionic concentrations in the selectivity filter. As bath $Ca^{2+}$ is increased to micromolar concentrations, $Na^+$ is replaced by $Ca^{2+}$ in the selectivity filter. The replacement is half complete at 1 $\mu$M bath $Ca^{2+}$ (the dielectric coefficient was chosen to match this apparent dissociation constant). In this graph, the $Cl^-$ curve is indistinguishable from the baseline. (*B*) Free energies of partitioning $\Delta G_i$ for $Ca^{2+}$, $Na^+$, and $Cl^-$ vary as the ionic compositions in the bath (and hence the selectivity filter) are varied. $\Delta G_i = \mu_i^{ex} - \mu_{0,i}^{ex} + z_i e_0 \Psi$, where *i* identifies the type of ion and $\Psi$ (note lower case) is the relative Donnan potential (filter/bath). (*C*) Differences of ionic excess chemical potentials (filter/bath) vary only weakly as $Ca^{2+}$ replaces $Na^+$ in the selectivity filter. The offset between the (relative) excess chemical potential of $Ca^{2+}$ and the (relative) excess chemical potential of $Na^+$ varies even less. (*D*) Donnan electric potential at the filter/bath junction varies strongly as $Ca^{2+}$ replaces $Na^+$ in the selectivity filter. The variation in electrical potential has important effects on $Ca^{2+}/Na^+$ selectivity because the Donnan potential has differential effects on the electrical energy of divalent and monovalent ions. The free energy of $Ca^{2+}$ partitioning (*panel B*) varies more strongly than that of $Na^+$ partitioning because the electrical energy of $Ca^{2+}$ varies twice as much as the electrical energy of $Na^+$.

3. Compute the ionic densities in the filter, $\rho_i$, from the Boltzmann relations

$$k_B T \ln \rho_i(m+1) = k_B T \ln \rho_{0,i} + \mu_{0,i}^{ex} - z_i e_0 \Psi(m) - \mu_i^{ex}(m); \quad (30)$$

4. Solve the MSA to compute the excess chemical potentials $\mu_i^{ex}$ for all ion species in the selectivity filter, including the selectivity oxygen ions. These excess chemical potentials are used to update those from the preceding (*m*th) iteration $\mu_i^{ex}(m)$ by the formula

$$\mu_i^{ex}(m+1) = \frac{\alpha \mu_i^{ex}(m) + \mu_i^{ex}}{1+\alpha} \quad (31)$$

The lag factor $\alpha$ is needed to ensure stability (typically $\alpha = 5$) because the ionic densities in the filter are exponential functions of the excess chemical potentials there. In some rare situations, $\alpha$ was as large as 100;

5. Update the electrical potential in the filter using the formula

$$\Psi(m+1) = \Psi(m) + \Delta\Psi \quad (32)$$

The iterative variation of the potential $\Delta\Psi$ depends on the charge and ionic densities in the selectivity filter $\rho_i$, including the selectivity oxygens.

$$\Delta\Psi = \frac{\sum_i z_i \rho_i}{\sum_i z_i^2 \rho_i} \quad (33)$$

The potential from the $m$th iteration thus is changed by an amount proportional to the remaining deviation from electroneutrality, but the size of the change is controlled by the ratio of the deviation from electroneutrality to the ionic strength in the selectivity filter;

6. If $|\Delta\Psi| > eps$, the iteration is done again from step 3 above. Otherwise, the calculation is stopped; $eps$ is a convergence criterion, typically $10^{-8}$.

## Solving the MSA

The solution of the MSA is given by a set of algebraic equations, but involves one iterative loop to determine the screening parameter $\Gamma$. We use a simple iteration with $m$ as the index. The MSA equations used for the selectivity filter have been defined above.

1. Set the screening parameter $\Gamma$ to an initial value $\Gamma(m = 0) = \kappa/2$;
2. Compute a new estimate $\Gamma(m + 1)$ for the screening parameter from Eq. 7 using the previous estimate $\Gamma(m)$ on the right-hand side of the equation;
3. Apply a convergence criterion: if $|\Gamma(m + 1) - \Gamma(m)|/\Gamma(m) > eps$, where $eps = 10^{-8}$, reiterate from step 2; otherwise proceed to step 4;
4. Compute the electrostatic part of the excess chemical potentials from Eq. 16. Compute the excluded volume part of the excess chemical potentials from Eq. 19. Combine the electrostatic and excluded volume parts to compute the total excess chemical potentials by Eq. 12.

The MSA was solved for both the bath and selectivity filter. The computation for the filter used fixed ionic diameters and a permittivity that was supplied as an external parameter. Selectivity oxygens were assigned the partial charge (valence) $-\frac{1}{2}e_0$. Crystal diameters (in nm) are given in Table 1.

The computation for the baths used concentration-dependent ionic diameters and a concentration-dependent permittivity. The diameters and permittivity were calculated as described by Simonin et al. (1996) and Simonin (1997) using coefficients from Table 2 of Simonin, 1997. The concentration dependence of these parameters adds additional terms in the excess chemical potentials, beyond those given in Eqs. 16 and 19. The full expressions used for bath calculations are found in Simonin, 1997 (his equations 1 and 4).

## RESULTS

Fig. 1 *A* shows our image of the hypothesized selectivity filter, i.e., binding site, 0.5 nm long and ~1 nm in diameter. The filter is formed by the narrowest constriction of a transmembrane pore, and more than ¼ of its volume is filled by oxygen ions and their counterions (Fig. 1 *B*). These oxygens are thought to belong to the four glutamate residues of the EEEE locus and are held in the filter by their tethers, that is, by the covalently linked atoms of the acid side and main chains. The tethers only act to localize the selectivity oxygens in this model. The oxygens and conducted ions in the selectivity filter behave like a concentrated (10–20 M) ionic solution on the biologically relevant time scale (>1 $\mu$s). The tethers do not add to the free energy of ion binding in any other way in this model. The ions in the filter are assigned crystal diameters (Table 1) and are drawn to scale. The oxygen ions are given the diameter of water oxygens as determined in hydration shells of ions (0.278 nm; Table 1). Each oxygen carries a charge of $-\frac{1}{2}e_0$. Water molecules in the filter and solutions outside the filter are not shown in the sketch. A volume of physiological bath solution (~0.1 M), equal to the volume of the filter, contains ~12 water molecules. The MSA screening radius computed for the concentrated solution in the filter is less than the oxygen radius (Fig. 1 *C*).

**TABLE 1 Ionic diameters**

| $Li^+$ | $Na^+$ | $K^+$ | $Rb^+$ | $Cs^+$ | $Mg^{2+}$ | $Ca^{2+}$ | $Ba^{2+}$ | $Cl^-$ | $O^{-1/2}$ |
|---|---|---|---|---|---|---|---|---|---|
| 0.148 | 0.204 | 0.276 | 0.298 | 0.340 | 0.144 | 0.200 | 0.272 | 0.362 | 0.278 |

Values are given in nm. Effective diameters for coordination number VI were taken from Shannon, R. D. and C. T. Previtt (1969). The diameter of $O^{-1/2}$ is the best estimate of oxygen in hydration shells found in Marcus, 1988.

$Ca^{2+}$ binding in L-type calcium channels is inferred from measurements of the current or conductance of the membranes of whole cells or of membrane patches containing a single channel. The channel bathed in a pure NaCl solution has a large conductance, and adding $CaCl_2$ to one or both baths reduces the (time or population) average of conductance approximately as described by a first-order isotherm (Kostyuk et al., 1983; Almers et al., 1984). At ~1 $\mu$M external $Ca^{2+}$, current between −20 to 0 mV is reduced to half its maximal value. The isotherm is thought to reflect the entry of $Ca^{2+}$ into the selectivity filter. Current or conductance is reduced because $Ca^{2+}$ is less mobile than $Na^+$. Following this lead, we assume that the selectivity filter holds equal charges (not amounts) of $Na^+$ and $Ca^{2+}$ when it is at the midpoint of the current isotherm. We choose values of the filter volume and dielectric coefficient that produce equal amounts of charge at the midpoint of the isotherm. The filter volume usually had the dimensions shown in Fig. 1 *A*, 0.5 nm long and ~1 nm in diameter (volume 0.375 $nm^3$), and the theory was calibrated to data by adjusting only the dielectric coefficient, which is 63.5 for the volume 0.375 $nm^3$.

This paper focuses on the competition among alkali and alkali earth ions, and the anion $Cl^-$, and is restricted to the roles of electrostatic screening and excluded volume effects in this competition. The chemical binding of protons to carboxylate ions, which results in conduction block, is not included in the present description. Thus, all computations apply to low proton concentrations (pH > 9).

Fig. 2 *A* shows the filter concentrations of $Na^+$ and $Ca^{2+}$ computed for an experiment in which $CaCl_2$ is added to a 0.1 M NaCl bath solution. $Ca^{2+}$ replaces $Na^+$ as the counterion in the filter as $Ca^{2+}$ is added to the bath. The theory predicts exchange isotherms with a midpoint at 1 $\mu$M bath $Ca^{2+}$ when the dielectric coefficient is set to 63.5 and the volume of the filter is 0.375 $nm^3$. This result shows that electrostatics and core-core repulsion can produce selective binding of $Ca^{2+}$ and $Na^+$ that varies with concentration like that in a real $Ca^{2+}$ channel. We will show below that the model produces a wide range of selectivities if we assign different values to the filter volume or dielectric coefficient.

The isotherms in Fig. 2 *A* have slopes smaller than in a first-order hyperbola because the free enthalpy of partitioning varies with the bath concentration of $Ca^{2+}$ (Fig. 2 *B*). As $Ca^{2+}$ is increased, selectivity is reduced, mostly because of changes in the long-range electrical (Donnan) potential between the filter and bath compartments (Fig. 2 *D*). Differences in the binding of different ions are reduced.

The concentration of $Ca^{2+}$ in the bath has little effect on the other, local components of the free energy: the filter-bath differences in excess chemical potentials for each ion are approximately independent of bath concentration (Fig. 2 *C*). The Donnan potential and approximately constant differences of excess chemical potentials of cations computed using MSA theory are in good agreement with previous empirical estimates obtained from a PNP model of the L-type calcium channel (Nonner and Eisenberg, 1998). The MSA computation also gives an estimate of the excess chemical potential for $Cl^-$ (Fig. 2 *C*); this potential is more repulsive than was postulated previously.

The $Ca^{2+}$-dependent reduction of $Na^+$ current through $Ca^{2+}$ channels has been previously described by a first-order isotherm (Kostyuk et al., 1983; Almers and McCleskey, 1984; Almers et al., 1994), so it is interesting to see if the experimental observations are compatible with the different kind of isotherm that we compute. Fig. 3 *A* replots the data of Almers and McCleskey (1984, their Fig. 11) together with a theoretical curve (*solid line*) computed from a Poisson-Nernst-Planck model (PNP2) of the $Ca^{2+}$ channel (Nonner and Eisenberg, 1998; see also legend to Fig. 3), usually called the self-consistent drift-diffusion equations in physical chemistry (Newman, 1991) and semiconductor physics (Ashcroft and Mermin, 1976; Hess, 2000).

PNP2 describes the flux of ions produced by the mean electrochemical gradient, including the mean electric field computed from all the charges in the system.

The PNP2 theory of the $Ca^{2+}$ channel involves a long-range (Donnan) potential similar to that computed in the present work (Figs. 2 and 4 *A* of Nonner and Eisenberg, 1998), and thus variable free energies of ion binding. The excess chemical potentials assigned to individual ions in the PNP2 model (their Table 1: 4 carboxyls) are constants, however, whereas they are variables in the MSA theory of the present paper. The numerical values of these constants in the PNP2 model are similar to the approximately constant excess chemical potential produced by the MSA theory (see our Fig. 2 *B*). Therefore, the PNP2 model produces the same kind of binding curves as we find here using MSA theory. A summary of theoretical binding curves has been published by Dang and McCleskey (1998, their Fig. 1) for three chemical-kinetic models that involve first-order binding with fixed free enthalpies. Fig. 4 *A* of the present paper shows the curve computed from our PNP2 model superimposed on the experimental points of Almers and McCleskey (1984). The curve computed from PNP2 theory follows the data more accurately than those of the kinetic models,

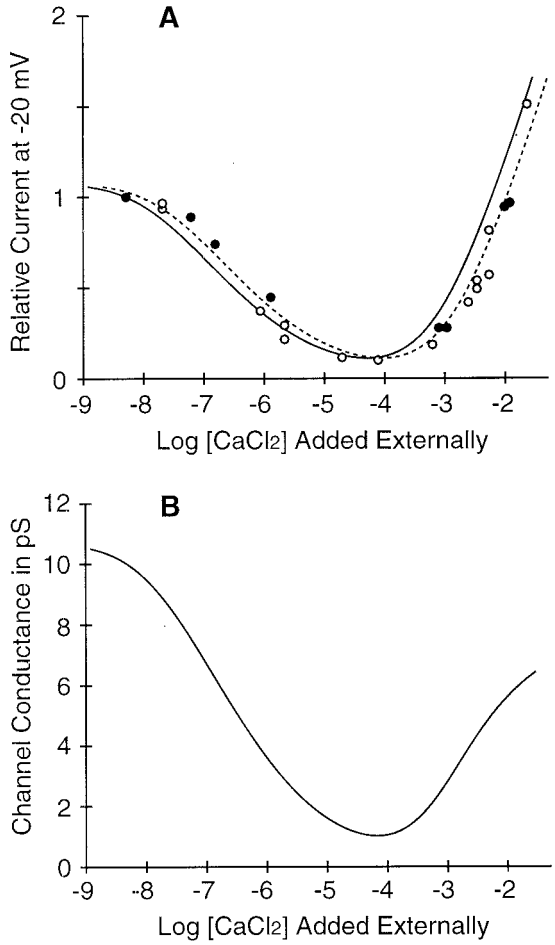


FIGURE 3 Selective ion binding incorporated in a model of conduction. (*A*) Comparison of experimental and theoretical currents through $Ca^{2+}$ channels. Symmetrical solutions of 30 mM $Na^+Cl^-$, 130 mM $TMA^+$ $Cl^-$ (tetramethylammonium chloride), pH 7. Calcium was added to the external bath as indicated on the abscissa. Symbols represent experimental measurements from Almers and McCleskey (1984; their Fig. 11; points that represent averages are filled). The solid curve is computed from the PNP2 model of Nonner and Eisenberg (1998) with the model parameters given in their Table 1 (4 carboxylate groups); TMA was assumed to be excluded from the pore proper by an excess chemical potential of 0.5 eV. Experimental points were measured from a whole cell containing an unknown number of channels. Theoretical currents were computed for a single channel and scaled to the leftmost experimental point. Note that the solid curve is a prediction, not a least-squares fit of the data: the parameters of this model describe idealized key observations derived from single-channel experiments and were not readjusted for these data. The dashed curve was obtained by shifting the predicted solid line along the abscissa. (*B*) Predicted channel conductance. The curve was computed from the PNP2 model of Nonner and Eisenberg (1998) and corresponds to the currents shown by the solid line in *panel A.* It has a distinct minimum of conductance, the so-called anomalous mole fraction effect of conductance.

although this curve was not obtained by a fit of the shown data: the model was calibrated using idealized measurements on single $Ca^{2+}$ channels as described in Nonner and Eisenberg (1998). A small horizontal shift of the predicted curve (*dashed line*) is enough to fit these specific data.

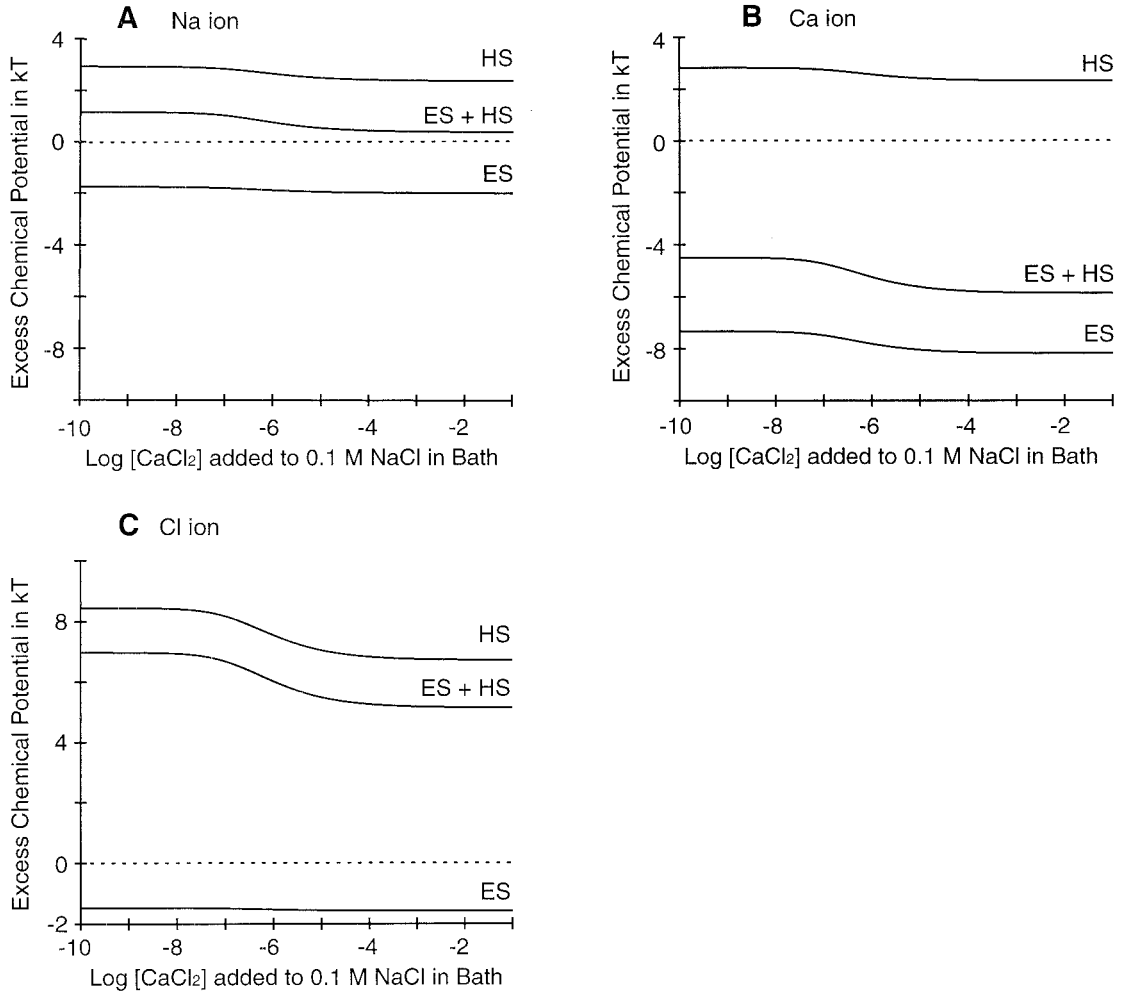


FIGURE 4 Components of the ionic excess chemical potentials in the selectivity filter in the $Ca^{2+}/Na^{+}$ replacement experiment of Fig. 2. For each ionic species the hard-sphere (HS) and electrostatic (ES) contributions to the total (ES + HS) excess chemical potentials are plotted. The hard-sphere excess potentials of $Na^{+}$ and $Ca^{2+}$ are similar and repulsive, but the electrostatic excess potential is much more attractive for $Ca^{2+}$ than for $Na^{+}$. The hard-sphere excess potential for $Cl^{-}$ is strongly repulsive, and that repulsion dominates the weaker attractive electrostatic excess potential for $Cl^{-}$. The ES components of excess chemical potential are computed from Eq. 16 and the HS components from Eq. 19, using the crystal ionic diameters (Table 1).

Chemical kinetic descriptions of the $Ca^{2+}$ channel in fact have two binding affinities for $Ca^{2+}$. In addition to high-affinity $Ca^{2+}$ binding (kD $\sim$ 1 $\mu$M), a domain of low-affinity $Ca^{2+}$ binding (kD $\sim$ 10 mM) was introduced into these models to predict an increase of current observed when the bath $Ca^{2+}$ reaches millimolar concentrations (Almers and McCleskey, 1984; Hess et al., 1986). Because the current reaches a minimum near $10^{-4}$ M $Ca^{2+}$, this has been called an anomalous mole fraction effect, AMFE. Our PNP2 computations reproduce the experimental AMFE of current (Fig. 3 *A*) and predict an AMFE of conductance (Fig. 3 *B*), as well. This AMFE is produced by depletion of $Ca^{2+}$ in the microscopic boundary layers at the filter/bath interfaces (Nonner and Eisenberg, 1998) and does not involve a separate low-affinity binding site. Instead, these small zones of low-affinity binding arise necessarily at the edges of an otherwise uniform filter region.

## Selectivity involves both electrostatic and excluded volume effects

Fig. 4 shows how electrostatic screening (ES) and excluded volume effects among hard spheres (HS) contribute to the individual excess chemical potentials in the hypothesized filter. The repulsive HS contributions are nearly identical for $Na^{+}$ and $Ca^{2+}$ because of their similar diameters. The charges on $Na^{+}$ and $Ca^{2+}$ are different, so their ES contributions are different enough to produce a substantial difference in the overall excess chemical potential and binding. The overall excess chemical potential for $Na^{+}$ is dominated by HS repulsion and thus is mildly repulsive. The overall excess chemical potential for $Ca^{2+}$ is dominated by the ES contribution, and thus attractive. The difference in the total excess chemical potential for $Ca^{2+}$ and $Na^{+}$ represents the chemically specific properties of the system. These arise

entirely from the interplay of electrostatics and core-core repulsion.

The origin of the different ES contributions for $Na^+$ and $Ca^{2+}$ can be traced through the MSA equations. The electrostatic (ES) component of the individual excess chemical potentials depends on the square of the valency and the ionic diameter, e.g., Eq. 16. The electrostatic component of the excess chemical potential for $Ca^{2+}$ is about four times that for $Na^+$ (Fig. 4, *A* and *B*), given that these ions have about the same diameter. When ions have different diameters, electrostatic selection also involves the ionic diameter (see Fig. 6). The hard-sphere (HS) contribution to the excess chemical potentials increases superlinearly with ionic density (Eq. 19), and becomes substantial when $>1/4$ of the space is filled by the ions, as in our system (Fig. 1 *B*). Thus, replacing 4 $Na^+$ by 2 $Ca^{2+}$ substantially reduces the excluded volume, changing the core-core repulsion and the HS free energy of the filter (also see the curve $-T\Delta S^{HS}$ in Fig. 9 *A*).

## Selectivities for other ions

It is interesting to see what predictions are made for other selectivities after our model has been tuned to give an appropriate $Ca^{2+}/Na^+$ selectivity. We predict selectivities using independently known crystal diameters of ions, so no adjustable parameters are involved. Figs. 5 and 6 give computations for alkali and alkali earth ions.

Fig. 5 *A* plots the concentrations of alkali metal cations at various concentrations of $Ca^{2+}$ in the bath. As the $Ca^{2+}$ in the bath is changed, the concentrations of the alkali metal ions in the selectivity filter change differently depending on the alkali ion present. Selectivity is seen. Indeed, the vari-

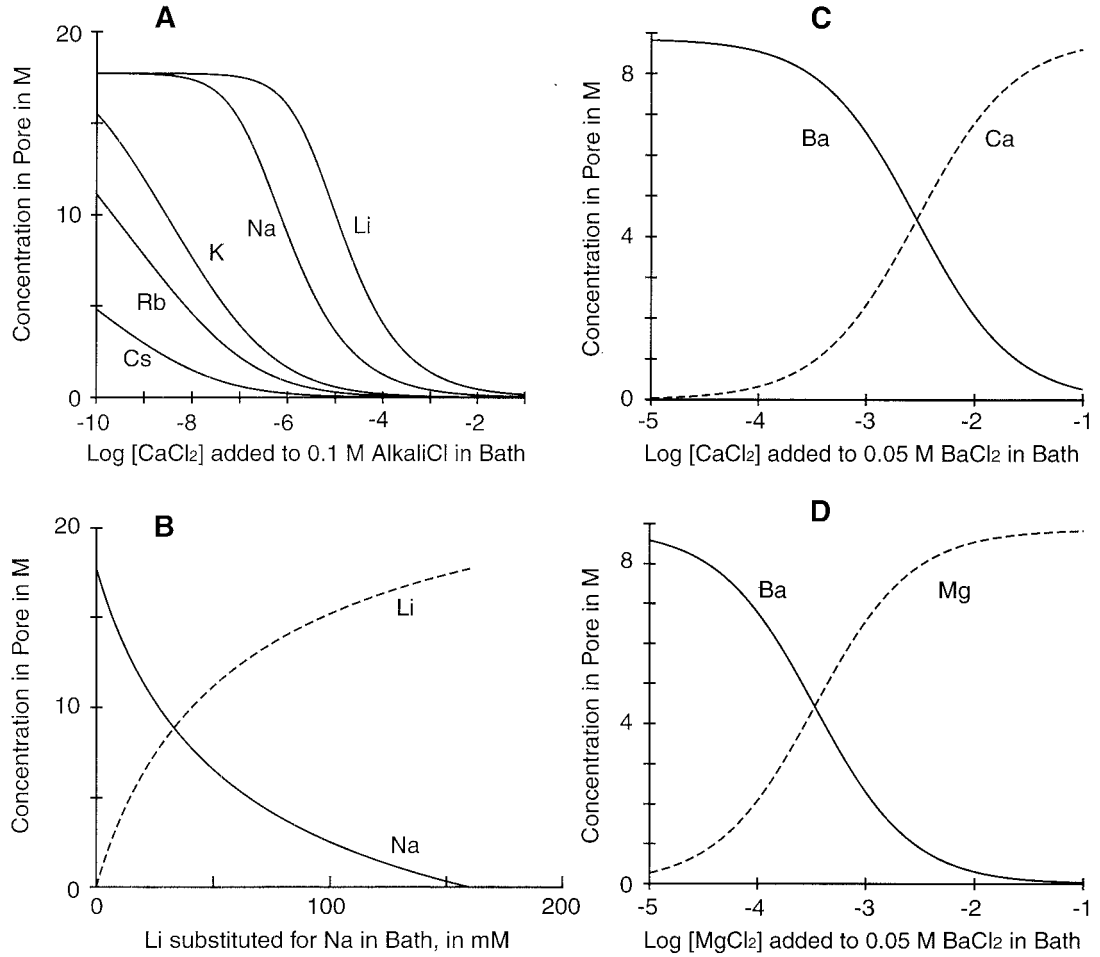


FIGURE 5 Predicted selectivities of alkali ions and $Ba^{2+}$. (*A*) Replacement of alkali cations by $Ca^{2+}$ added as $CaCl_2$ to 0.1 M alkali $Cl^-$ in bath. (*B*) Replacement of $Na^+$ by $Li^+$ by varying the mole fraction of $Li^+$ in 0.16 M sodium/lithium mixtures in the bath. (*C*) Replacement of $Ba^{2+}$ by $Ca^{2+}$ added as $CaCl_2$ to 50 mM $BaCl_2$ in the bath. (*D*) Replacement of $Ba^{2+}$ by $Mg^{2+}$ added as $MgCl_2$ to 50 mM $BaCl_2$ in the bath. Note that these computations do not invoke additional adjustable parameters beyond the parameters of the selectivity filter used in Fig. 2. All ionic diameters were set at their published crystal values (see Theory and Methods).

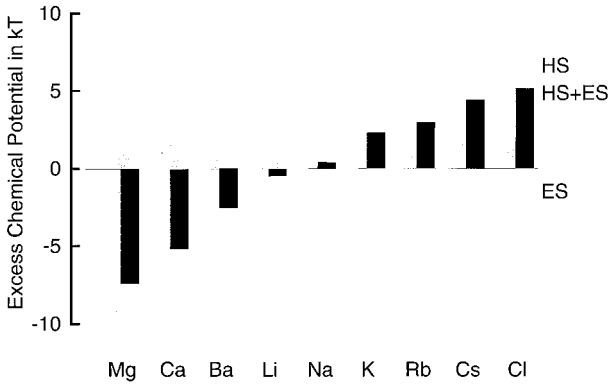


FIGURE 6 Determinants of selectivity in the hypothesized filter. Excess chemical potentials (*black columns*) are the algebraic sums of hard-sphere contributions (HS, shown in *dark gray columns*) and electrostatic contributions (ES, shown in *light gray columns*). The potentials shown were computed for a filter saturated with $Ca^{2+} \sim 9$ M.

ations predicted in Fig. 5 *A* seem larger than those that have been observed in experiments. The binding curves imply a striking reduction of $Cs^+$ and $K^+$ currents by very low $Ca^{2+}$ that seems to disagree with experimental finding of large $Cs^+$ or $K^+$ currents in the presence of $Ca^{2+}$ chelators (Pietrobon et al., 1989). However, the experimentally found block of $Li^+$ inward current occurs at a few micromolar $Ca^{2+}$, which is less than predicted. [The $Ca^{2+}$ concentration needed depends on the direction of current and the side of calcium application (Kuo and Hess, 1993)]. These experimental observations were made using $Ca^{2+}$ chelators to establish the desired low bath concentrations of $Ca^{2+}$ in the presence of a large background concentration of monovalent salt. Their buffered solutions were designed using binding constants that were adjusted for ionic strength, but not for the concentrations of specific alkali metal ions. If these chelators (which involve four carboxylate groups, like the EEEE locus) themselves are selective with respect to alkali cations, the above experiments would be sensitive only to differences between the cation selectivities of the $Ca^{2+}$ channel and of the chelators of the $Ca^{2+}$ buffer.

$Ca^{2+}$ chelation typically involves several carboxylate groups that are tethered together into one molecule. Our MSA computations show how such chelators can have a high $Ca^{2+}$ affinity, and they suggest that an attached fluorophore could function as a $Ca^{2+}$ indicator if it senses and reports the long-range electric field that emanates from the carboxylate/$Ca^{2+}$ mixture nearby. We imagine that the long-range electric field in the fluorophore varies with the concentration of free $Ca^{2+}$ in the solution, much as does the electric field of the selectivity filter shown in Fig. 2 *D*. The aromatic rings of the fluorophore (of the chelator) extend through much of that field and their absorption or fluorescence would change as the field changes.

Other observations made on ionic competition in $Ca^{2+}$ channels do not depend on the accuracy of buffered $Ca^{2+}$ concentrations. Prod'hom et al. (1989, their Fig. 5) measured single-channel conductance in mixtures of $Na^+$ and $Li^+$. The mixture of 20 mM $Li^+$ and 140 mM $Na^+$ gave a conductance about halfway between the conductances in pure $Li^+$ or $Na^+$ solutions. Fig. 5 *B* plots the concentrations of $Na^+$ and $Li^+$ in the hypothesized filter, computed for these ionic conditions. The midpoint of the "replacement curve" is at $\sim$30 mM $Li^+$, in good agreement with the observation. Lansman et al. (1986, their Fig. 8) measured currents in the presence of 50 mM $Ba^{2+}$ while adding a varied concentration of $Ca^{2+}$. The transition between the current levels observed in pure solutions is half complete at $\sim$3 mM $Ca^{2+}$. The simulated filter concentrations for $Ba^{2+}$ and $Ca^{2+}$ (Fig. 5 *C*) are in good agreement with their experimental findings.

Fig. 6 summarizes how selective binding to various ions arises in the hypothesized filter. For each species, the excluded volume HS and electrostatic ES contributions are shown by shaded columns, and the net excess chemical potentials are shown as a superimposed solid column. Note that these potentials were computed for a filter containing mostly $Ca^{2+}$ as the counterion of the oxygen ions, as one would expect under physiological conditions. These potentials would be quite different if other ions were in the filter, because the potentials depend on the composition of the entire system.

Negative (i.e., attractive) excess chemical potentials arise for the divalent cations, $Ca^{2+}$ and $Ba^{2+}$, and for the monovalent cation $Li^+$. The repulsive excluded volume terms of these three ions are not as large as the strong electrostatic terms because of their double valency and/or small ionic diameter. Alkali metal cations larger than $Li^+$ have positive (repulsive) excess chemical potentials due to their smaller electrostatic and larger excluded volume effects.

Specificity of $Ca^{2+}$ over $Mg^{2+}$ is important for calcium channels and other calcium-selective proteins because their $Ca^{2+}$-dependent functions are performed in the presence of millimolar concentrations of $Mg^{2+}$. In L-type calcium channels, 10 mM external $Mg^{2+}$ half-blocks $Ba^{2+}$ inward currents in the presence of 50 mM external $Ba^{2+}$, and 3 $\mu$M external $Mg^{2+}$ blocks $Li^+$ inward currents in 300 mM external $Li^+$ (Kuo and Hess, 1993). These observations suggest that the affinity of the channel for $Mg^{2+}$ is slightly less than for $Ca^{2+}$. When we simulate such experiments using the crystal diameter of $Mg^{2+}$, half-saturation concentrations for $Mg^{2+}$ are predicted to be smaller by an order of magnitude than those for $Ca^{2+}$. A more appropriate $Mg^{2+}$ selectivity would be obtained using an effective $Mg^{2+}$ diameter of $\sim$0.25 nm rather than the crystal diameter of 0.144 nm. This anomaly with regard to $Mg^{2+}$ will be discussed below.

Conduction in L-type calcium channels is blocked by very low concentrations of some transition metal cations, such as $Cd^{2+}$. About 10 $\mu$M external $Cd^{2+}$ blocks half of the inward currents supported by 50 mM external $Ba^{2+}$ (Lansman et al., 1986), and $\sim$1 nM $Cd^{2+}$ blocks currents in the presence of 0.1 M $Li^+$ (Ellinor et al., 1995). $Cd^{2+}$ and

$Ca^{2+}$ have nearly the same crystal diameters. Thus, a 1000-fold higher binding affinity for $Cd^{2+}$ over $Ca^{2+}$ cannot be accounted for in terms of the electrostatic and excluded volume interactions computed by the MSA, nor as a hydration effect. About 7 $k_BT$ beyond the MSA figure are needed to account for $Cd^{2+}$ binding; such attractive effects likely involve strong dispersion or other quantum-mechanical coordination characteristic of transition metals like cadmium (Baes and Mesmer, 1976; Magini et al., 1988).

## Selectivity over a range of oxygen ion densities and dielectric coefficients

Fig. 7 *A* shows the effects of varying the volume of the selectivity filter from the reference value of 0.375 $nm^3$. The bath concentration of $Ca^{2+}$ needed to displace half of the $Na^+$ is increased by ~10-fold when the volume is increased by 40%; it is reduced more than a hundredfold when the filter volume is reduced by 40%. Fig. 7 *B* shows the effects of different dielectric coefficients (between 40 and 80). In the primitive MSA model, dielectric coefficients include hydration/solvation effects.

Fig. 7 *C* shows the values of the filter volumes and dielectric coefficients that combined give the observed midpoint of the Na/Ca replacement curve, 1 $\mu$M. For instance, a filter volume smaller than our 0.375 $nm^3$ can produce a calcium/sodium replacement curve with midpoint at 1 $\mu$M bath $Ca^{2+}$ if the dielectric coefficient is increased. The volume has to be within a certain range if the theory is to fit data. If the volume is increased twofold (and a lower di-

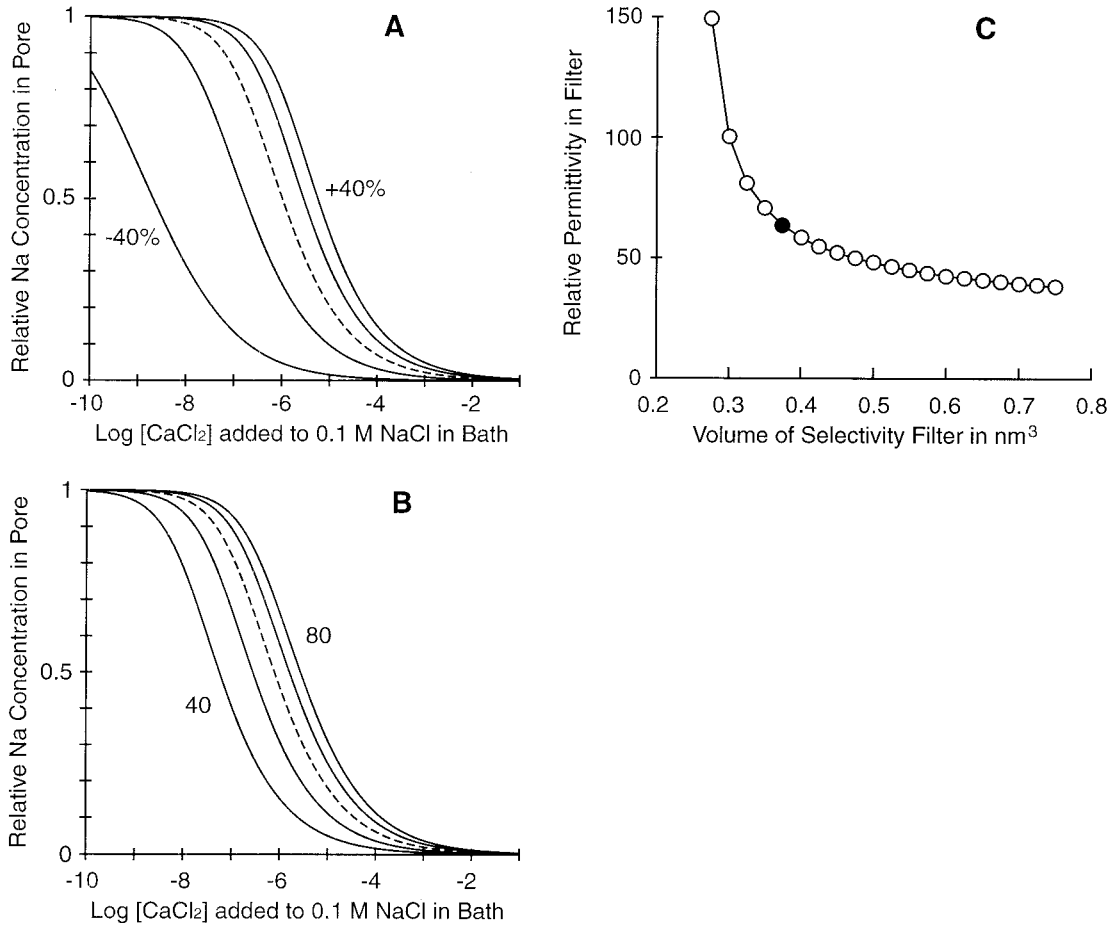


FIGURE 7 Effects on selectivity of (*A*) changes of filter volume or (*B*) changes of effective dielectric coefficient. The volume of the hypothetical selectivity filter is varied in steps of 20% from the reference value, 0.375 $nm^3$ (*dashed curve*). The dielectric coefficient is varied in steps of 10 between 40 and 80 (the *dashed curve* is for 60). The curves give the relative $Na^+$ concentration (with respect to the carboxyl concentration) remaining in the selectivity filter when $CaCl_2$ is added to 0.1 M NaCl in the bath. Small increases of the volume of the selectivity filter shift the calcium/sodium curve to the right and have effects similar to small increases of the dielectric coefficient. (*C*) Dielectric coefficients and filter volumes that when combined produce the physiological calcium/sodium selectivity (one half of the $Na^+$ in the filter is replaced by $Ca^{2+}$ when $[Ca^{2+}]$ in the bath is 1 $\mu$M). The filled symbol marks the standard dielectric coefficient and filter volume. Selection by electrostatic screening increases from left to right, whereas selection by excluded volume effects decreases in the same direction. Filters of large volume reject anions weakly (compare Fig. 8, *A* and *B*).

electric coefficient 38 is chosen to allow fit to the replacement data), $Cl^-$ is bound in the filter (Fig. 8 *A*) and thus would be conducted by the channel. $Cl^-$ can enter when the volume is large because hard-sphere repulsive effects are then reduced. The ions have more room. The reduced value of the dielectric coefficient required by the increased value of the volume (as specified in Fig. 7 *C*) strengthens electrostatic attraction for all ions, leading also to a positive long-range potential (Fig. 8 *B*).

However, reduction of the filter volume to 0.2 $nm^3$ requires very large dielectric coefficients to fit the 1 $\mu$M midpoint of the $Na^+/Ca^{2+}$ replacement curve. If the dielectric coefficient is set to 80, the replacement midpoint is drastically shifted to lower bath $Ca^{2+}$, and a complete $Ca^{2+}/Na^+$ replacement requires many orders of magnitude of variation in bath $Ca^{2+}$ (Fig. 8, *C* and *D*), differing in both respects from the properties of the real channel. $Cl^-$ repulsion is enhanced under these conditions due to the strong

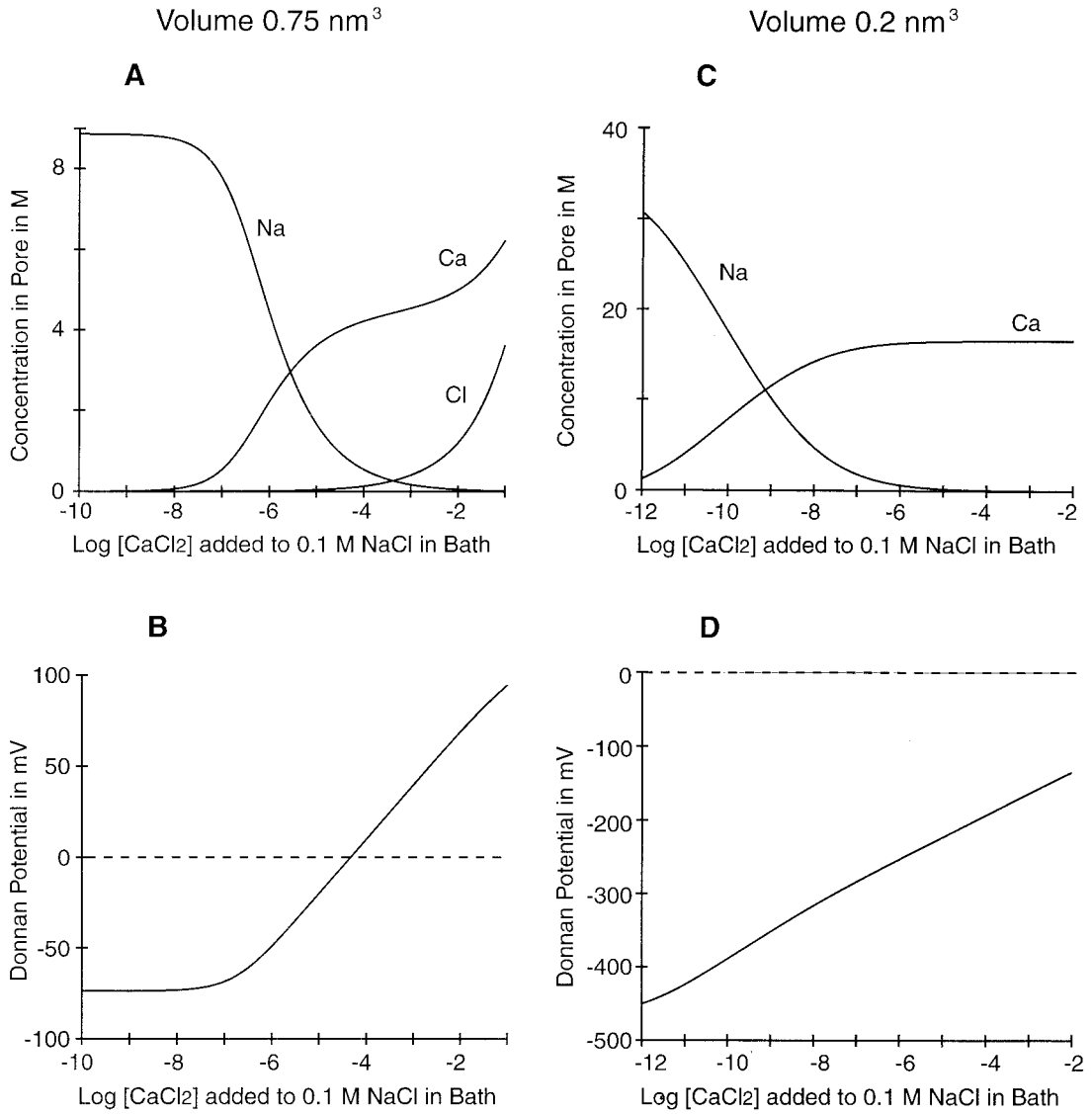


FIGURE 8 Effects of excessively large or small filter volumes. The oxygen ions are confined in filter volumes of 0.75 $nm^3$ (*A* and *B*) or 0.2 $nm^3$ (*C* and *D*), about twice or one-half the standard volume. If the effective dielectric coefficient is set to 38, the large filter volume (low density of selectivity oxygens) is compatible with the actual midpoint of $Ca^{2+}/Na^+$ replacement, but other properties become unrealistic. The large filter volume and reduced dielectric coefficient increase electrostatic effects and reduce excluded volume effects. These produce a positive electrostatic potential (the Donnan potential $\Psi$) and allow for a substantial concentration of $Cl^-$ in the selectivity filter. Thus, $Cl^-$ rejection is compromised and the hypothetical channel is on its way to becoming an anion channel (see Appendix of Nonner and Eisenberg, 1998). The small filter volume (high oxygen density) requires dielectric coefficients much larger than 80 to give an appropriate midpoint for the $Ca^{2+}/Na^+$ replacement. With the dielectric coefficient set to 80, the midpoint of the replacement occurs at bath $Ca^{2+}$ levels of $\sim 10^{-10}$ M, so $Ca^{2+}/Na^+$ selectivity is much higher than in the real channel. In the proposed MSA theory, physiological selectivity arises when the selectivity oxygens are neither too concentrated nor too dilute.

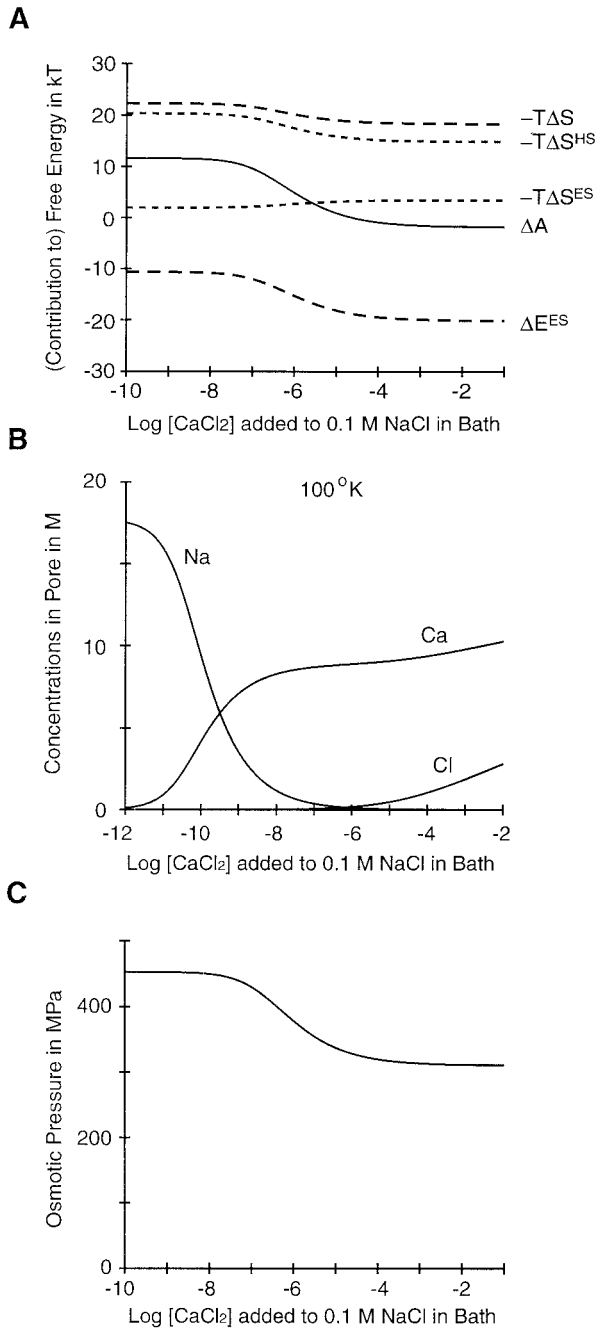


FIGURE 9 (*A*) Thermodynamic balance sheet of $Ca^{2+}$ selectivity. *Curve A* shows the Helmholtz excess free energy of all the ions in the hypothesized selectivity filter taken together, both the selectivity oxygens and the mobile species. $\Delta A$ has an electrostatic component $\Delta E^{ES}$, and an entropic contribution, $-T\Delta S$. The entropy change is negative and arises from the separation of co and counterions when electrostatic screening occurs ($-T\Delta S^{ES}$) and from the mutual exclusion of ions that have a finite hard-sphere diameter ($-T\Delta S^{HS}$). The entropic expense involved in electrostatic screening is small compared to entropic effects resulting from volume exclusion. It is also small compared to the gain in electrostatic energy. The internal electrostatic energy term and the total entropic term are of opposite signs: electrostatic attraction is opposed by entropic repulsion of mobile ions. When $Ca^{2+}$ is replaced by $Na^+$ in the selectivity filter, both components of excess free energy change in the negative direction. The change in the total free energy is larger (in magnitude) than either component alone: electrostatic internal energy and entropy act together in promoting the selection of $Ca^{2+}$ over $Na^+$. (*B*) Calcium binding predicted at ~100 K. In the cold, the midpoint of the calcium/sodium replacement curve is shifted to the left by 4 orders of magnitude. Compare with Fig. 2. Selectivity is greatly enhanced at low $Ca^{2+}$ concentrations. At physiological $Ca^{2+}$ concentrations, $Cl^-$ is found in the selectivity filter, which is not present at biological temperatures. Parameters are the same as those used in Figs. 1 and 2. (*C*) Osmotic pressure. The high ionic concentrations and substantial hard-sphere effects generate a high osmotic pressure. The pressure decreases from left to right in the graph, as $Ca^{2+}$ is added to the bath, as 2 $Ca^{2+}$ replace 4 $Na^+$. Parameters are those used in Figs. 1 and 2.

excluded volume effects and a strong negative Donnan potential (Fig. 8 *D*).

## DISCUSSION

The MSA model of specific ionic binding in $Ca^{2+}$ channels described here is remarkably simple. Long-range electrostatic and excluded volume interactions among mobile ions and partially charged oxygens of carboxylate groups of the protein suffice to produce a range of selectivities, dependent on the volume density of oxygen ions and the dielectric conditions. This selectivity arises in a setting of minimal structure, where ions and tethered structural groups interact like molecules in a homogeneous solution without preordained structure. The protein supplies only a volume, dielectric constant, and selectivity oxygens. Solvation is described implicitly in this model by the dielectric properties assigned to the filter and bath solutions.

The hypothesized selectivity filter distinguishes between $Na^+$ and $Ca^{2+}$ by two effects: 1) divalent $Ca^{2+}$ screens the structural oxygen ions more effectively than monovalent $Na^+$, and thus has a more negative (attractive) electrostatic potential there (Figs. 2, 4, and 9 *A*). 2) Four $Na^+$ displace about twice the volume of two $Ca^{2+}$, producing a repulsive excess potential for $Na^+$ (Fig. 1 *B*). With electroneutrality as a dominating constraint, the selectivity filter can use volume exclusion to distinguish ions of nearly the same diameter, such as $Na^+$ and $Ca^{2+}$, because *equal charge excludes different volumes depending on the valency of the mobile ion.* In this way, electrostatics facilitates selection by volume exclusion: substantial repulsion due to excluded volume selects against $Na^+$ (and other monovalent cations) compared to $Ca^{2+}$ (Fig. 6).

The specific interactions inside the hypothesized filter are reflected in the long-range (Donnan) potential that extends from the filter into the baths. When $Ca^{2+}$ is present in the filter, the carboxylate ions are strongly screened and the long-range field is weak. When only $Na^+$ is available in the bulk solution, screening inside the filter is weaker and the long-range field is stronger. It is the long-range field that then attracts $Na^+$ or any other available cation into the filter when divalents are absent, and only monovalents are available to satisfy electroneutrality.

The hypothesized filter selects also against anions such as $Cl^-$ (Fig. 4 *C*). Experiments have shown that particles larger than $Cl^-$ actually can pass through $Ca^{2+}$ channels (McCleskey and Almers, 1985). MSA theory reveals that the rejection of $Cl^-$ is not a trivial consequence of negative structural charge. Surprisingly, the electrostatics of negatively charged groups alone cannot repel anions over the entire range of bath $Ca^{2+}$. The stronger the electrostatics in the filter, the more $Cl^-$ is predicted to partition into the filter when $CaCl_2$ concentration is raised in the bath (Fig. 8 *A*). The $Ca^{2+}$/oxygen-ion mixture in the filter then attracts $Ca^{2+}$ by a low excess chemical potential and it attracts $Cl^-$ by the resulting positive long-range (Donnan) potential (Fig. 8 *B*), much as the surface of a growing salt crystal attracts both cations and anions in equivalent amounts. $Cl^-$ can be rejected only when excluded volume effects are substantial. Then, $Cl^-$ itself is repelled from the filter due to its large diameter, and a positive long-range potential cannot arise because local screening of the oxygen ions by $Ca^{2+}$ is reduced by excluded-volume interactions (compare Fig. 2). In the selectivity against $Cl^-$, it is volume exclusion that facilitates selection by electrostatics, whereas in the selectivity against $Na^+$, it is the electrostatics that facilitates selection by volume exclusion.

## Parameters of the MSA model

With ions assigned fixed (crystal) diameters, affinities for physiological ions are chosen to fit experiment by adjusting the value of dielectric coefficient in the selectivity filter. The ionic density in the selectivity filter is determined by the fixed density of structural charge, and so the dielectric coefficient was assumed to be constant independent of bath composition. A second free parameter defines the unknown volume accessible to the tethered carboxylate oxygens in the filter. This volume also is taken as constant and thus unaffected by bath composition. The two free parameters have global roles in the model.

The filter volume sets ionic density and thus controls the strengths of both Coulombic and excluded volume effects. The dielectric coefficient independently scales the strength of electrostatic effects, and thus is able to balance attractive (electrostatic) against the repulsive (excluded volume) effects. Experimental observations on $Ca^{2+}/Na^+$ and other selective ion/ion exchanges in calcium channels are described using reasonable settings of these global parameters (Figs. 2 *A*, 5 *B* and *C*). When comparing the selectivity filter of the theory with bulk solution, one should note that the MSA description of a 6 mol/l $CaCl_2$ solution involves a dielectric coefficient of 37.6 (Simonin, 1997), in line with experimental results in concentrated solutions (Barthel et al., 1995). Excluded volume effects in 6 mol/kg-$H_2O$ $CaCl_2$ solution produce an experimental osmotic coefficient of 2.891 (Robinson and Stokes, 1959). We compute a value of ~6.65 for the osmotic coefficient of the 9 mol/l $Ca^{2+}$ carboxylate solution that is the selectivity filter of our model.

The electrochemical potential consists of many components, for example, the Donnan electrical potential, the ideal chemical potential, the hard-sphere potential of uncharged spheres, and the excess electrostatic potential of the MSA, which in turn have entropy and energy components. Each component is different for each ion and may vary in different ways, as the concentration of ions is changed in the bath. Thus, a *large repertoire of behavior can arise in this simple system, available to be exploited by evolution in biologically useful ways.* The selectivities described in this model arise as a generic property of carboxylate/ion interactions. Such selectivities could have evolved in any system that has large ionic densities, large excluded-volume effects, and Coulombic interactions moderated by the dielectric. Evolution could enforce and modulate selectivity simply by setting the filter volume and effective dielectric constant and volume of the selectivity filter.

Excluded volume effects arise here chiefly from the tethered carboxylate groups, which we have represented as two separate oxygen atoms with a charge of $-1/2$ each. While electrostatics thus might be described quite well (with intercarboxylic oxygen distances approaching intracarboxylic distance), we might expect to underestimate excluded-volume effects of the rather bulky side chains of glutamate residues. We also may have ignored excluded-volume contributions from other uncharged side chains in the pore, or ionic packing restricted by confinement. To the extent that such conditions exist in the real pore, our model requires larger than actual densities of groups (a smaller volume), with the side effect that electrostatics are overestimated. Model optimization would yield a larger than actual dielectric coefficient (see Fig. 7 *C*). However, it must be remembered that the dielectric coefficient in our primitive MSA description is an effective parameter that concatenates at least two physical effects, one the change in solvation energy associated with moving an ion from the bath to the filter, and the other the attenuation of electrostatic interactions in a medium containing induced (i.e., dielectric) charge. These two contributions to the electrostatic energy are of opposite sign; their difference seems to be important in determining the net effect on selectivity, and so an explicit treatment of solvation in the solution and in the filter will be needed before the value of the local dielectric coefficient can be reliably estimated.

Although the MSA model appears satisfactory for most physiological ions, it does not predict an appropriate $Ca^{2+}/Mg^{2+}$ selectivity (experimental $Mg^{2+}$ affinity is described only if $Mg^{2+}$ is assigned a diameter larger than the crystal diameter). Experimental stability constants of carboxylate-cation associations in bulk solutions are similar for $Mg^{2+}$ and $Ca^{2+}$, and chelators involving several carboxylate groups tend to select $Ca^{2+}$ over $Mg^{2+}$ (Dawson et al., 1987). In the $Ca^{2+}$ binding site of galactose-binding protein,

ionic affinities increase with decreasing ionic diameter for divalent and trivalent cations, but the smallest ion studied in each group, $Mg^{2+}$ and $Sc^{3+}$, break the trend (Drake et al., 1997). Low $Mg^{2+}$ affinity thus appears generic for carboxylate-based binding sites. It seems plausible that oxygens in tethered carboxylate groups are sterically more impeded in screening a very small ion than are the oxygens of bulk water.

### Thermodynamics of the selectivity filter

Fig. 9 *A* plots the Helmholtz excess free energy and its components, computed for the ensemble of our standard model as it undergoes $Ca^{2+}/Na^{+}$ exchange. The excess free energy (curve $\Delta A$) is positive when the filter contains $Na^{+}$, and turns negative as $Ca^{2+}$ enters. Both entropic ($T\Delta S$) and energy ($\Delta E^{ES}$) contributions to the free energy vary substantially under these conditions, both favoring the entry of $Ca^{2+}$. The entropic contribution involves the hard-sphere effect ($T\Delta S^{HS}$) and a small term related to creating the ionic screening arrangements in a real solution ($T\Delta S^{ES}$).

$T\Delta S^{ES}$ is the energetic cost of screening arrangements that form spontaneously, and it is this term that is expected to be reduced if, e.g., carboxylate ions had been positioned in a specific spatial structure for optimal interaction with $Ca^{2+}$. Both the electrostatic energy gained in screening as well as the repulsive excluded-volume work are substantially larger than the entropic work involved in screening. Spontaneous "coordination" as modeled here can underlie a range of selectivities, including those of $Ca^{2+}$ channels (Fig. 7, *A* and *B*). Our computations thus do not support the notion that a specific three-dimensional atomic structure is crucial for selectivity in $Ca^{2+}$ channels.

Although crystallographic structures of $Ca^{2+}$ channels are currently unavailable, $Ca^{2+}$-binding motifs of other proteins have been resolved. Typically, they involve a central $Ca^{2+}$ in contact with seven oxygen atoms of carboxylate and other groups (e.g., the motif of galactose-binding protein, Vyas et al., 1987), but there appears to be substantial variability in the conformations and organizations of EF-hand sites (Nelson and Chazin, 1998). It is not clear to what extent these three-dimensional structures, which apply to crystallographic temperatures, relate to physiological function. MSA theory can estimate temperature dependency of ion binding (Blum and Rosenfeld, 1991). Even if filter volume and dielectric coefficient are assumed to be constant, the theoretical screening radii are reduced to ~0.08 nm at 100 K, so a $Ca^{2+}$ charge is screened by a virtual sphere of countercharge only ~0.18 nm in radius. Crystallographic $Ca^{2+}$-oxygen distances average 0.241 nm and water is essentially excluded from the complex (Vyas et al., 1987). Our MSA computations reveal substantial changes in binding characteristics. Cooling calcium channels to 100 K is predicted to increase $Ca^{2+}/Na^{+}$ selectivity $10^4$-fold (Fig. 9 *B*). Low temperature enhances attractive effects due to electrostatic energy, but does not affect repulsion by the entropic excluded-volume effects. Thus, it has a large net effect on binding.

Substantial excluded volume effects in a molecular pore raise the question of mechanical stability. An upper limit for the force exerted on the channel wall is given by the osmotic pressure that the filter contents would produce in a classical macroscopic Donnan system (Fig. 9 *C*). This pressure is very large. When the contents of the selectivity filter change, e.g., when $Na^{+}$ is replaced by $Ca^{2+}$, osmotic pressure also changes substantially. The pressure of 400 MPa corresponds to a force of 200 pN in the wall of pore of the dimensions given in Fig. 1 *A*, and this force varies by ~50 pN when $Na^{+}$ is exchanged for $Ca^{2+}$. The force would be substantially larger with a large counterion (such as $Cs^{+}$), so it is conceivable that the pore dimensions increase under such ionic conditions. Mechanical forces of this kind might underlie $Ca^{2+}$-induced conformational changes in calcium-regulated proteins, but the mechanical energy terms are necessarily ignored until a theory of the inhomogeneous system, e.g., Density Functional Theory (Rosenfeld and Blum, 1986; Henderson, 1992; Frink and Salinger, 1999), is developed, along with estimates of the electromechanical properties of channel and other proteins.

We are deeply indebted to Professor Lesser Blum, who has spent innumerable hours and much effort teaching us the MSA. It is a pleasure to thank Karl Magleby for his advice and support and to thank him, Ellen Barrett, Gavriel David, and Tom DeCoursey for their critical reading of the manuscript. We are grateful to a referee for significant support and useful suggestions.

This work was supported by National Institutes of Health Grant GM30377 (to W.N.) and Defense Advanced Research Projects Agency Grant N65236-98-1-5409 (to B.E.).

## REFERENCES

Almers, W., and E. W. McCleskey. 1984. Non-selective conductance in calcium channels of frog muscle: calcium selectivity in a single-file pore. *J. Physiol.* 353:585–608.

Almers, W., E. W. McCleskey, and P. T. Palade. 1984. Non-selective cation conductance in frog muscle membrane blocked by micromolar external calcium ions. *J. Physiol.* 353:565–583.

Armstrong, C. M. 1989. Reflections on selectivity. *In* Membrane Transport: People and Ideas. D. C. Tosteson, editor. American Physiological Society and Oxford University Press, New York.

Ashcroft, N. W., and N. D. Mermin. 1976. Solid State Physics. Harcourt Brace College Publishers, New York.

Baes, C. F., Jr., and R. E. Mesmer. 1976. The Hydrolysis of Cations. Wiley, New York.

Barthel, J., R. Buchner, and M. Münsterer. 1995. Electrolyte Data Collection Vol. 12, Part 2: Dielectric Properties of Water and Aqueous Electrolyte Solutions. DECHEMA, Frankfurt am Main, Germany.

Bernard, O., and L. Blum. 1996. Binding mean spherical approximation for pairing ions: an exponential approximation and thermodynamics. *J. Chem. Phys.* 104:4746–4754.

Berry, S. R., S. A. Rice, and J. Ross. 1980. Physical Chemistry. John Wiley & Sons, New York.

Blum, L. 1975. Mean spherical model for asymmetric electrolytes I: method of solution. *Mol. Phys.* 30:1529–1535.

Blum, L. 1980. Solution of the Ornstein-Zernike equation for a mixture of hard ions and Yukawa closure. *J. Stat. Phys.* 22:661.

Blum, L., and J. S. Hoye. 1977. Mean spherical approximation for asymmetrical electrolytes II: thermodynamic properties and the pair correlation function. *J. Phys. Chem.* 81:1311–1316.

Blum, L., Y. K. Kalyuzhnyi, O. Bernard, and J. N. Herrera-Pacheco. 1996. Sticky charged spheres in the mean-spherical approximation: a model for colloids and polyelectrolytes. *J. Phys.: Condens. Matter*. 8:A143–A167.

Blum, L., and Y. Rosenfeld. 1991. Relation between the free energy and the direct correlation function in the mean spherical approximation. *J. Stat. Phys.* 63:1177–1190.

Boda, D., D. Henderson, and K.-Y. Chan. 1999. Monte Carlo study of the capacitance of the double layer in a model molten salt. *J. Chem. Phys.* 110:5346–5350.

Coster, H. G. L. 1973. The double fixed charge membrane. *Biophys. J.* 13:133–142.

Coster, H. G. L., E. P. George, and R. Simons. 1969. The electrical characteristics of fixed charge membranes: solution of the field equations. *Biophys. J.* 9:666–684.

Dang, T. X., and E. W. McCleskey. 1998. Ion channel selectivity through stepwise changes in binding affinity. *J. Gen. Physiol.* 111:185–193.

Dawson, R. M. C., D. C. Elliot, W. H. Elliott, and J. K. M. 1987. Data for Biochemical Research, Chap. 17. Oxford, New York.

Drake, S., M. Zimmer, C. Kundrot, and J. Falke. 1997. Molecular tuning of an EF-hand-like calcium binding loop. Contributions of the coordinating side chain at loop position. *J. Gen. Physiol.* 110:173–184.

Eisenman, G., and R. Horn. 1983. Ionic selectivity revisited: the role of kinetic and equilibrium processes in ion permeation through channels. *J. Membr. Biol.* 76:197–225.

Ellinor, P. T., J. Yang, W. A. Sather, J.-F. Zhang, and R. Tsien. 1995. $Ca^{2+}$ channel selectivity at a single locus for high-affinity $Ca^{2+}$ interactions. *Neuron.* 15:1121–1132.

Frink, L. J. D., and A. G. Salinger. 1999. Density Functional Theory for Classical Fluids at Complex Interfaces. Sandia National Laboratory, Albuquerque, New Mexico. 1–77.

Heinemann, S. H., H. Terlau, W. Stuhmer, K. Imoto, and S. Numa. 1992. Calcium channel characteristics conferred on the sodium channel by single mutations. *Nature.* 356:441–443.

Helfferich, F. 1962. Ion Exchange. McGraw Hill, New York.

Henderson, D. 1992. Fundamentals of Inhomogeneous Fluids. Marcel Dekker, New York.

Hess, K. 2000. Advanced Theory of Semiconductor Devices. IEEE Press, New York.

Hess, P., J. F. Lansman, and R. W. Tsien. 1986. Calcium channel selectivity for divalent and monovalent cations. *J. Gen. Physiol.* 88:293–319.

Hess, P., and R. W. Tsien. 1984. Mechanism of ion permeation through calcium channels. *Nature.* 309:453–456.

Hille, E., and W. Schwartz. 1978. Potassium channels as multi-ion single-file pores. *J. Gen. Physiol.* 72:409–442.

Kostyuk, P. G., S. L. Mironov, and Y. M. Shuba. 1983. Two ion-selective filters in the calcium channel of the somatic membrane of mollusc neurons. *J. Membr. Biol.* 76:83–93.

Kuo, C. C., and P. Hess. 1993. Block of the L-type $Ca^{2+}$ channel pore by external and internal $Mg^{2+}$ in rat phaeochromocytoma cells. *J. Physiol. (Lond.).* 466:683–706.

Lansman, J. B., P. Hess, and R. W. Tsien. 1986. Blockade of current through single calcium channels by $Cd^{2+}$, $Mg^{2+}$, and $Ca^{2+}$. Voltage and concentration dependence of calcium entry into the pore. *J. Gen. Physiol.* 88:321–347.

Lee, K. S., and R. W. Tsien. 1984. High selectivity of calcium channels as determined by reversal potential measurements in single dialyzed heart cells of the guinea pig. *J. Physiol. (Lond.).* 354:253–272.

Magini, M., G. Licheri, G. Piccaluga, G. Paschina, and G. Pinna. 1988. X-ray Diffraction of Ions in Aqueous Solutions: Hydration and Complex Formation. CRC Press, Boca Raton, FL.

Mandl, F. 1988. Statistical Physics. Wiley, New York.

Mansoori, G. A., N. F. Carnahan, K. E. Starling, and T. W. Leland, Jr. 1971. Equilibrium thermodynamic properties of the mixture of hard spheres. *J. Chem. Phys.* 54:1523–1525.

Marcus, Y. 1988. Ionic radii in aqueous solutions. *Chem. Rev.* 88: 1475–1498.

McCleskey, E. W., and W. Almers. 1985. The Ca channel in skeletal muscle is a large pore. *Proc. Natl. Acad. Sci. USA.* 82:7149–7153.

Mikala, G., A. Bahinski, A. Ytani, S. Tang, and A. Schwartz. 1993. Differential contribution of conserved glutamate residues to an ion-selectivity site in the L-type $Ca^{2+}$ channel pore. *FEBS Lett.* 335: 265–269.

Miller, C. 1999. Ionic hopping defended. *J. Gen. Physiol.* 113:783–788.

Nelson, M., and W. Chazin. 1998. Structures of EF-hand $Ca^{2+}$-binding proteins: diversity in the organization, packing and response to $Ca^{2+}$ binding. *Biometals.* 11:297–318.

Newman, J. S. 1991. Electrochemical Systems. Prentice-Hall, Englewood Cliffs, NJ.

Nonner, W., and B. Eisenberg. 1998. Ion permeation and glutamate residues linked by Poisson-Nernst-Planck theory in L-type calcium channels. *Biophys. J.* 75:1287–1305.

Onsager, L. 1939. Electrostatic interactions of molecules. *J. Phys. Chem.* 63:189–196.

Pietrobon, D., B. Prod'hom, and P. Hess. 1989. Interactions of protons with single open L-type calcium channels. *J. Gen. Physiol.* 94:1–21.

Prod'hom, B., D. Pietrobon, and P. Hess. 1989. Interactions of protons with single open L-type calcium channels. *J. Gen. Physiol.* 94:23–42.

Reuter, H., and H. Scholz. 1977. A study of ion selectivity and the kinetic properties of the calcium dependent slow inward current in mammalian cardiac muscle. *J. Physiol. (Lond.).* 264:49–62.

Robinson, R. A., and R. H. Stokes. 1959. Electrolyte Solutions. Butterworths Scientific Publications, London.

Rosenfeld, Y., and L. Blum. 1986. Statistical mechanics of charged objects: general method and application to simple systems. *J. Chem. Phys.* 85:1556–1566.

Salacuse, J. J., and G. Stell. 1982. Polydisperse systems: statistical thermodynamics, with applications to several models including hard and permeable spheres. *J. Chem. Phys.* 77:3714–3725.

Shannon, R. D., and C. T. Previtt. 1969. Effective ionic radii in oxides and fluorides. *Acta Crystallog.* B25:925–946.

Simonin, J.-P. 1997. Real ionic solutions in the mean spherical approximation. 2. Pure strong electrolytes up to very high concentrations and mixtures, in the primitive model. *J. Phys. Chem. B.* 101:4313–4320.

Simonin, J.-P., O. Bernard, and L. Blum. 1998. Real ionic solutions in the mean spherical approximation. 3. Osmotic and activity coefficients for associating electrolytes in the primitive model. *J. Phys. Chem. B.* 102: 4411–4417.

Simonin, J.-P., L. Blum, and P. Turq. 1996. Real ionic solutions in the mean spherical approximation. 1. Simple salts in the primitive model. *J. Phys. Chem. B.* 100:7704–7709.

Teorell, T. 1953. Transport processes and electrical phenomena in ionic membrane. *Prog. Biophys. Mol. Biol.* 3:305–369.

Triolo, R., L. Blum, and M. A. Floriano. 1978a. Simple electrolytes in the mean spherical approximation II: study of a refined model. *J. Phys. Chem.* 82:1368–1370.

Triolo, R., L. Blum, and M. A. Floriano. 1978b. Simple electrolytes in the mean spherical approximation III: a workable model for aqueous solutions. *J. Chem. Phys.* 67:5956–5959.

Triolo, R., J. R. Grigera, and L. Blum. 1976. Simple electrolytes in the mean spherical approximation. *J. Phys. Chem.* 80:1858–1861.

Vyas, N. K., M. N. Vyas, and F. A. Quiocho. 1987. A novel calcium binding site in the galactose-binding protein of bacterial transport and chemotaxis. *Nature (Lond.).* 327:635–638.

Yang, J., P. T. Ellinor, W. A. Sather, J. F. Zhang, and R. Tsien. 1993. Molecular determinants of $Ca^{2+}$ selectivity and ion permeation in L-type $Ca^{2+}$ channels. *Nature.* 366:158–161.